WESTERN SYDNEY
UNIVERSITY

School of Medicine

Sutureless repair of transected nerves using photochemically bonded collagen membranes

Master of Science (Honours) Medicine thesis

Zoran Pletikosa

BMed, MHSc (Ed)

Supervisor:

Professor John Morley

Cosupervisor:

Dr David Mahns

Sydney 2018

Statement of Authentication

The work presented in this thesis is, to the best of my knowledge and belief, original except as acknowledged in the text. I hereby declare that I have not submitted this material, either in full or in part, for a degree at this or any other institution.

Zoran Pletikosa

Table of contents

Abstract

Peripheral nerve injuries are relatively common with broad-ranging aetiologies that often produce debilitating functional consequences. In its most severe form, nerve trauma involves complete transection of the nerve causing denervation of the target tissue with corresponding functional deficit. While the body possesses an ability to regenerate the severed axons through the mechanism of axon budding, such process is generally incomplete and fails to fully restore sensory and/or motor functions. The outcomes are, among other things, influenced by the surgical repair technique used. For example, standard surgical approach involves suturing the approximated nerve ends, which does not always ensure good alignment and leads to retention of permanent non-absorbable suture material, which often leads to intraneural scarring. Here I have tested a novel sutureless nerve repair technique using a biodegradable collagen membrane bonded with a photochemically activated dye. This process avoids the tissue tension/compression and foreign material retention commonly associated with non-absorbable sutures. In a transected rat sciatic nerve model, this technique has demonstrated superior histological and functional recovery when compared to a standard suturing approach. In future it may form a viable and, potentially, better alternative for surgical treatment of nerve injuries in clinical practice. Additional research will be required to further quantify functional sensory and motor recovery process, as well as histological changes and outcomes in regard to inflammation and regeneration.

1. Introduction

1.1 Nerve anatomy

The peripheral nervous system is mainly composed of functional cells neurons and their axons, and supportive glia cells, which are largely Schwann cells. The function of neurons is to carry electrical signals between the central nervous system and the tissues, while the Schwann cells structurally support the axons, increase the speed of the electrical conduction and assist with axonal growth and regeneration after injury. A peripheral nerve is composed of one or more fascicles, which are bundles of myelinated and unmyelinated axons surrounded by a layer of strong protective connective tissue called perineurium (Fig. 1). Individual axons inside the fascicles are wrapped in a thin delicate connective tissue sheath called the endoneurium. The epineurium is the outer connective tissue layer covering all fascicles and binding them together. Generally, the greater the number of fascicles present in a peripheral nerve, the thicker the epineurium. Extending along the epineurium are the blood vessels that branch from regional arteries to supply the nerve. These vessels are interconnected with the network of small blood vessels found between and within the fascicles, forming a system of the vasa nervorum. Epineurial blood vessels are more susceptible to trauma than the deeper vessels of the nerve due to their more peripheral location and thus exposure to injury. But even the deeper vessels can be readily disrupted as a result of tension and/or compression that occur during the nerve repair (Clark et al. 1992, Schmidhammer et al. 2004).

1.2 Nerve injury

Peripheral nerve lesions are relatively common, affecting around 5% of trauma sufferers presenting to emergency departments (Robinson 2000). Nerve injuries can occur in different pathologic forms (Seddon 1975, Sunderland 1975). In neurapraxia the axons are preserved but unable to transmit impulses due to focal loss of myelin. In axonotmesis, the axons are damaged or destroyed, with variable damage of the connective tissue framework, but the nerve is still in anatomical continuity. In neurotmesis the nerve trunk is disrupted with most of the nerve connective tissue lost or badly distorted (Table 1).

Following transection of a nerve trunk, the axon segments distal to the lesion undergo a series of changes collectively known as Wallerian degeneration, starting within 24-48 hours following injury (Caillaud et al. 2019). In this process axoplasmic cytoskeleton disintegrates, Schwann cells lose the myelin portion of their membranes, and together with bone-marrow derived macrophages start to remove the degenerated axons and myelin (Chen, Piao & Bonaldo 2015, Rotshenker 2011, Zigmond & Echevarria 2019). Clearance of degenerated myelin is essential for repair as its prolonged presence inhibits successful regeneration of severed axons (McKerracher et al. 1994, Schwab 1996). For the first few days after injury Schwann cells are responsible for most phagocytic activity, until recruited monocytes accumulate in sufficient numbers (Gaudet, Popovich & Ramer 2011). After the removal of myelin debris, the proliferating Schwann cells align themselves into bands of Büngner, forming hollow tubes that provide a path for the axon sprouting from the proximal stump to grow into. This is a critical event in the repair process as some sprouts may become misdirected while others are stopped by the developing connective tissue. Axons that regenerate distally through erroneous pathways fail to reach their natural targets and consequently undergo degeneration (Brushart et al. 1998). Those axons that manage to connect with their tissue targets have smaller diameter, reduced conduction velocity and excitability for long time (Navarro, Vivo & Valero-Cabre 2007), which helps explaining inadequate functional recovery of reinnervated tissues.

In neurotmesis developing after lacerations or gunshot wounds, incomplete long term recovery with partial or total loss of motor and/or sensory functions is expected in the majority of patients (Panagopoulos, Megaloikonomos & Mavrogenis 2017, Palispis & Gupta 2017). As a rule, spontaneous recovery after neurotmesis does not occur. If a surgical repair is performed, some degree of clinical recovery will be observed, but it will not be complete, despite advances in microsurgical materials and methodologies. The success of nerve repair is dependent on regenerated motor, sensory and autonomic axons establishing functional connections with their distal targets. This is greatly influenced by the employed repair technique, as well as the expertise of the surgeon.

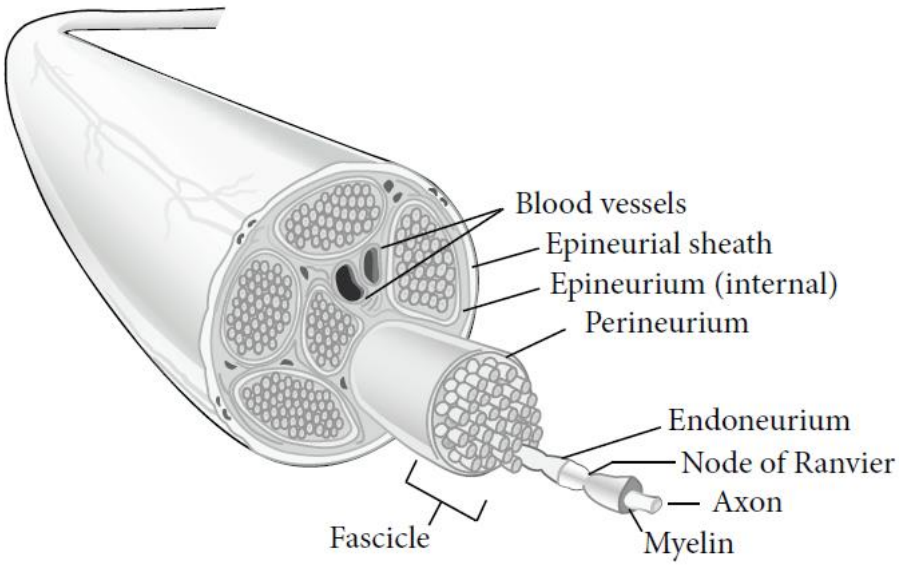

Figure 1: Peripheral nerve anatomy
(image from Grinsell & Keating 2014)

Seddon and Sunderland classifications of nerve injury

Seddon	Sunderland	Injury
Neurapraxia	Grade I	Focal segmental demyelination
Axonotmesis	Grade II	Axon damaged with intact endoneurium
Axonotmesis	Grade III	Axon and endoneurium damaged with intact perineurium
Axonotmesis	Grade IV	Axon, endoneurium, and perineurium damaged with intact epineurium
Neurotmesis	Grade V	Complete nerve transection

Table 1: Classification schemes of nerve injuries

1.3 Direct suturing in nerve injury repair

In surgical practice, the most commonly used method for repair of severed peripheral nerves involves epineurial suturing after the approximation of the nerve ends (neurorrhaphy). Suturing of individual fascicles or groups of fascicles has proven more time consuming and technically demanding. While in theory they offer better alignment of fascicles, in practice the clinical results are not superior (Millesi 2006).

Monofilament nylon suture is a preferred material for such work because of its ease of use and relatively small foreign-body reaction (Lee & Wolfe 2000). However, scarring cannot be fully avoided due to traumatic effects of the needle on the nerve tissue and retained non-absorbable sutures (Matsuyama, Mackay & Midha 2000, Yi & Dahlin 2010). Such scarring processes, which are well-recognised in the literature, interfere with the growth of regenerating axons across the injury site and may cause ischaemia by compressing the adjacent blood vessels (Ngeow 2010, Grinsell & Keating 2014, Menovsky & Beek 2003). Moreover, increased collagen production and poorer functional recovery have been associated with a greater number of sutures used at the repair site (Martins et al. 2011). Consequently, the fewest sutures capable of neurorrhaphy with good fascicular alignment are recommended (Siemionow & Brzezicki 2009). Additionally, tension exerted on the nerve ends by the placed sutures is often unavoidable due to nerve stump retraction after transection and surgical debridement of the nerve stumps before suturing. This tension has been demonstrated to significantly compromise intraneural microcirculation which negatively impacts on nerve regeneration (Abrams et al. 1998, Harris & Tindall 1991, Terzis, Faibisoff & Williams 1975).

From the research perspective nerve suturing technique is difficult to standardise which makes outcome measurements and comparisons difficult (Wang, Sunitha & Chung 2013). It has been observed that many surgeons show a tendency to apply the sutures too tightly in order to achieve a favourable appearance of the outer nerve surface, at the same time producing bunched up and misdirected fascicles inside (Isaacs 2013). For superior outcomes, the nerve ends should barely touch one another (Dahlin 2008), which requires more time and skill, and is consequently challenging in a busy surgical practice. A lack of subspecialty training

in microsurgery, and the insufficient experience and skills of surgeons are thus additional obstacles to satisfactory outcomes (Campbell 2008).

1.4 Conduits in nerve injury repair

Due to the aforementioned shortcomings of traditional surgical techniques, a number of alternative approaches have been investigated, among them prefabricated artificial tubes (conduits) are of particular interest (Jiang et al. 2010, Ciardelli & Chiono 2006, Pinho et al. 2016). It is important that such conduits have good biocompatibility, elasticity, porosity and biodegradability (Huang & Huang 2006). For direct nerve repair immediately after injury, short tubes have been employed as 'connectors' after the nerve stumps are placed a few millimetres into each end (Kannan et al. 2005). Sutures through the ends of the connector and epineurium are still required, but since fewer sutures are needed and they are positioned further away from the approximation line, there is less interference with axonal regeneration (Ducic, Fu & Iorio 2012). When using a nerve conduit, a small gap between the coapted nerve stumps is always left, which effectively avoids the fascicles in opposite nerve ends being compressed against one another. After acute transection such gap is quickly filled with a blood clot impregnated with fibrin matrix, providing a suitable medium for migration of macrophages and Schwann cells (Deumens et al. 2010). Additionally, a conduit around the injured nerve helps create a closed microenvironment from which axons are unable to escape, whilst connective tissue is prevented from invading the nerve, and growth factors can accumulate sufficiently to promote repair (Danielsen & Varon 1995). It has been postulated that conduit-based nerve repair materials have the potential to further advance and standardise nerve injury treatment (Bamba et al. 2017). Currently nerve conduits have been especially used for repair of short peripheral nerve defects as an alternative to autologous nerve grafts (Pabari et al. 2014). Their experimental and clinical evaluation is ongoing.

1.5 Sutureless techniques in nerve injury repair

In recent years, considerable research and development has been made using a sutureless nerve repair technique. Eliminating sutures should, in theory, minimise or avoid additional injury inflicted by tissue handling and needle penetration. This should result in reduced inflammatory reaction, less scarring and a better functional recovery, while at the same time

requiring less specialised surgical skills and experience. Potential added benefits are reduced surgical and recovery time, which would benefit both patient and surgeon.

Human and bovine fibrin tissue adhesives have been tried in animal models of primary repair of peripheral neurotmesis (Cruz, Debs & Fiol 1986, Félix et al. 2013, Koulaxouzidis, Reim & Witzel 2015, Suri, Mehta & Sarkar 2002). Fibrin adhesives are commercially available in two components, which, when mixed, start thrombin's enzymatic action on fibrinogen, resulting in formation of a sticky fibrin clot. This clot acts as an adhesive envelope to hold the cut nerve ends together, at the same time providing a barrier to connective tissue penetration into the nerve. The overall conclusion was that, in regard to functional recovery of transected nerves, performance of fibrin adhesive was equal, if not superior, to that of direct suturing (Sameem, Wood & Bain 2011). Additionally, it was observed that nerve repair performed with fibrin adhesive achieved histologically better fascicular alignment and axonal regeneration and generated less inflammation, fibrosis and neuroma formation (Ornelas et al. 2006, Menovsky & Beek 2001). The main disadvantage of fibrin adhesives in nerve repair appears to be the relative lack of tensile strength with a potential of bond failure (Temple et al. 2004).

Photochemical tissue bonding using a light-activated Rose-Bengal (RB) dye has been successfully tested to bond tissue interfaces directly (O'Neill et al. 2007, Yang et al. 2012) or with the use of covering material such as amniotic membranes (Fairbairn et al. 2016) and chitosan films (Lauto et al. 2005). Laser irradiation of RB has been found to be safe and well tolerated in vitro and in vivo (Yao et al. 2010). The exact chemical mechanism underlying the bonding process is not fully understood. However, it is postulated that the RB dye absorbs light energy and initiates release of reactive oxygen species, which cause covalent cross-linking between amino acids in collagen proteins (Kamegaya et al. 2005, Cherfan et al. 2013). Chitosan-RB films have attracted considerable attention due to their low-cost fabrication, easy use and favourable biocompatibility, inducing only minimal foreign body reaction (Rodríguez-Vázquez et al. 2015). Chitosan is a polysaccharide derived from deacetylated chitin and can be mixed with RB dye and readily cast in a thin film of around 20 µm thickness (Lauto et al. 2012). Transected nerves, repaired with a laser-activated chitosan-RB films, demonstrated at least equivalent histological and functional recovery results when compared to the standard suture repair (Barton et al. 2015). Nevertheless, photochemically bonded chitosan-RB films tend to detach from the underlying epineurium after several days, therefore

they cannot continue supporting the nerve repair over a longer period, and have limited biodegradability, which may be somewhat improved with modifying the structural properties (Hutmacher, Goh & Teoh 2001). Consequently, biodegradable materials that can bond to tissue using laser light are being investigated.

For example, various types of mammalian collagen based membranes (such as derived from intestinal and bladder submucosa, pericardium, peritoneum and dermis), commonly referred to as extracellular matrix (ECM), have been developed for clinical use and are commercially available, in form of dry sheets, from more than 20 companies. Such material has been found to be an excellent scaffold suitable for use in orthopaedic, cardiac and abdominal surgeries due to its effective structural support, biodegradability and ability to release biologically active factors that promote tissue healing and remodelling (Badylak, Freytes & Gilbert 2009, Lun et al. 2010, Benders et al. 2013). These collagen membranes are employed in the form of sheets that can be cut to size and then used for wrapping or covering of the injured tissue. After placement, the material is typically attached to the surrounding tissue with anchoring sutures.

Decellularisation (elimination of cells) during the ECM manufacturing process also removes antigens, which avoids clinically significant inflammatory response and immunological rejection (Parmaksiz et al. 2016). ECM major components such as collagen (mainly type I), fibronectin, laminin, elastin and glycosaminoglycans help mimic the native-like environment that can support cell proliferation and migration during repair (Rijal 2017). ECM biomaterials retain their structural characteristics at the site of implantation for 1-2 months, during which the matrix is slowly degraded and is incorporated into the endogenous ECM produced by resident fibroblasts (Gilbert et al. 2007). ECM component molecules released through the natural degradation process have been shown to enhance axonal regeneration and myelination during nerve repair (De Luca et al. 2015). ECM material wrapped around nerves is quickly vascularised in situ and gradually remodelled into the connective tissue structure similar to nerve epineurium (Kokkalis et al. 2011). It has even been demonstrated that biodegradable collagen membrane wrapped around a sutured nerve leads to significantly less adhesions with surrounding tissues (extraneural fibrosis) (Mathieu et al. 2012).

CelGro® is a relative newcomer to the market and is produced by Orthocell (Perth, Australia). It is a porcine peritoneum-derived collagen membrane which is currently TGA-approved and

CE-certified for use in assisting tympanic membrane, tendon, cartilage and bone regeneration in various surgical applications. In clinical trials CelGro was found to be well tolerated by the host tissue after implantation, with minimal inflammatory response (Shen et al. 2014). The method of producing CelGro involves mechanical removal of the fat, proprietary decellularisation process, dehydration and sterilisation by gamma irradiation. The material is commercially available in different thicknesses, depending on intended clinical application.

1.6 Behavioural and electrophysiological methods of studying nerve regeneration

In research of peripheral nerve regeneration rats constitute an invaluable animal model as they are relatively inexpensive and easily housed and handled. Additionally, rat nerves have similar morphology to human ones and are large enough to be subjected to standard microsurgical techniques. The rat sciatic nerve is the most commonly employed nerve in neuroscience research even though there are concerns about reliability of translating such outcomes to humans, especially in regard to gap injuries (Kaplan, Mishra & Kohn 2015). Rat sciatic nerve is composed of about 27,000 axons; 6% are myelinated motor axons, 23% and 48% are myelinated and unmyelinated sensory axons, respectively, and 23% are unmyelinated sympathetic axons (Schmalbruch 1986). Numerous motor and sensory functional assays have been established for investigations of its injury, repair and recovery (Nichols et al. 2005). While it is difficult to objectively compare them in regard to validity, some assays appear to be more popular than others.

Sciatic nerve and its branches supply the primary innervation of the rat hind limb and therefore functional motor deficit is apparent through changes in rat's gait (paw placement and stepping), as well as direct changes in limb strength. One of the most commonly used quantitative methods is walking track analysis of animal's footprints known as the sciatic functional index (SFI) (De Medinaceli et al. 1982). Walking track analysis is regarded as challenging and often burdened by technical problems in both performance and analysis. SFI is a reflection of complex integrated function, rather than being a pure test of sciatic motor function recovery (Bain, Mackinnon & Hunter 1989). Extensor postural thrust (EPT) test, as described by Thalhammer et al. (1995), measures the force exerted by the prime ankle plantar flexors (soleus and gastrocnemius, innervated by the sciatic nerve) on the digital platform scale. The test was found to be simple, easy to execute and requires virtually no computation

of results, while at the same time being indistinguishable from walking track analysis in regard to assessing motor recovery (Koka & Hadlock 2001). It should be noted that EPT does require substantial training for the tester to handle the animals in a comfortable manner, and to recognise when the animal is bearing its maximum weight on the tested hind limb. Without such experience the results can be unreliable and difficult to reproduce.

Electrophysiological investigations, especially compound muscle action potential (CMAP) recorded from the gastrocnemius muscle after sciatic nerve stimulation, are commonly used to evaluate the extent of sciatic regeneration. The CMAP represents a sum of motor unit activation under the recording electrode and its amplitude is proportional to the number of motor axons activated by the stimulating electrode placed over the nerve (Robinson 2000). Thus the amplitude of the CMAP evoked by nerve electrical stimulation is a reliable indicator of the number of regenerated large diameter myelinated Aα motor axons (Valero-Cabré et al. 2004, Campbell 2008). However, it has been reported that electrical activity in the gastrocnemius, after stimulation of the regenerating sciatic nerve, can also be contributed by surrounding hind limb muscles (biceps femoris and semimembranosus), unaffected by nerve injury (Rupp et al. 2007). Muscle electrophysiology becomes more reliable when correlated with measurement of gastrocnemius and soleus muscles weight. These two muscles operate as ankle plantar flexors and are innervated by the tibial branch of the sciatic nerve. The weight of muscles distal to nerve injury is generally proportional to the degree of innervation and thus constitutes a parameter for functional recovery (Evans et al. 1995). The effects of denervation on muscle weight develop quickly (denervation atrophy), while the recovery is slow, and is linked to progress of reinnervation (Navarro 2016).

Return of sensory perception is another important consideration in assessment of recovery from nerve injury. In practice it is very challenging to devise a pure sensory test. Since experimental animals, unlike humans, cannot communicate sensory perception, researchers must rely on motor responses to sensory stimuli, which typically are in a nociceptive range (algesimetry). Consequently, in such experimental assays it becomes impossible to separate sensory and motor function (Nichols et al. 2005). Nociception is typically evaluated by observing the withdrawal reflex of the hind limb in response to noxious stimulation which could be mechanical (electronic von Frey device, Casals-Díaz, Vivó & Navarro 2009) or thermal (focused radiant heat source, Hargreaves et al. 1988). It should be noted that pain

sensations are mainly transmitted via medium size myelinated Aδ fibres (first phase of pain, 'sharp' in nature), as well as unmyelinated small diameter C fibres (slow or 'burning' pain) (Bourne, Machado & Nagel 2014, Dubin & Patapoutian 2010). There is some evidence that at least some pain is transmitted via large myelinated Aβ fibres which generally carry information about touch, pressure, and vibration (Djouhri & Lawson 2004). Both Aβ fibres and C fibres have been implicated in development of mechanical allodynia after nerve injury (Finnerup 2011, Hulse, Wynick & Donaldson 2010, Jänig 2011).

Another issue to consider is that after sciatic nerve transection there is a preservation of sensation along the medial part of the foot innervated the saphenous nerve, a division of the femoral nerve. It has been demonstrated by Kingery & Vallin (1989) that collateral sprouting from the saphenous nerve into the tibial nerve (a division of the sciatic nerve) innervation territory start developing soon after sciatic nerve transection. Consequently, in order to avoid false positive results, testing of sensory recovery during sciatic nerve regeneration should be confined to the lateral aspect of the foot.

2. Aims and hypotheses

2.1 Aims

1. Assess the suitability of collagen membranes for photochemical bonding.

2. Compare the bonding properties of collagen membranes to those of chitosan-RB films.

3. Assess the suitability of collagen membranes for sutureless photochemical repair of transected nerves.

4. Compare the histological, electrophysiological and functional outcomes of collagen membrane repaired and suture repaired transected nerves.

2.2 Hypotheses

1. Collagen membrane can be photochemically bonded with Rose Bengal solution and green laser, and achieve comparable bonding strength to photochemically bonded chitosan-RB films.

2. Photochemically bonded collagen membranes are biocompatible and biodegradable.

3. Collagen membrane repaired nerves display improved electrophysiological and functional outcomes compared to suture repaired nerves.

4. Collagen membrane repaired nerves demonstrate less intraneural scarring and improved histology compared to suture repaired nerves.

3. Materials and methods

3.1 Collagen membrane biomaterial

CelGro collagen membrane was obtained from the manufacturer Orthocell (Murdoch, Australia) in a thickness of around 70±10 μm as measured with a digital micrometer (Mitutoyo, Japan) (Fig. 2). Such membrane was subjectively still very strong, effectively resisting tension in all directions, but also flexible to be easily wrapped around a small nerve. It is also easily cut to size with scissors or surgical scalpel. Due to the nature of the raw material used in its production, the membrane has a rough side (showing coarse collagen bundles) corresponding to submesothelial connective tissue, and a smooth but somewhat dimpled side corresponding to mesothelial surface (Fig. 3).

Rose-Bengal (RB) (Sigma-Aldrich, Australia) was prepared as 0.1% solution in sterile 0.9% saline. This concentration was found by Chan, Kochevar & Redmond (2002) to offer maximum bonding properties when exposed to laser light, which did not improve with further increase in RB concentration.

Figure 2: Macroscopic appearance of CelGro membrane

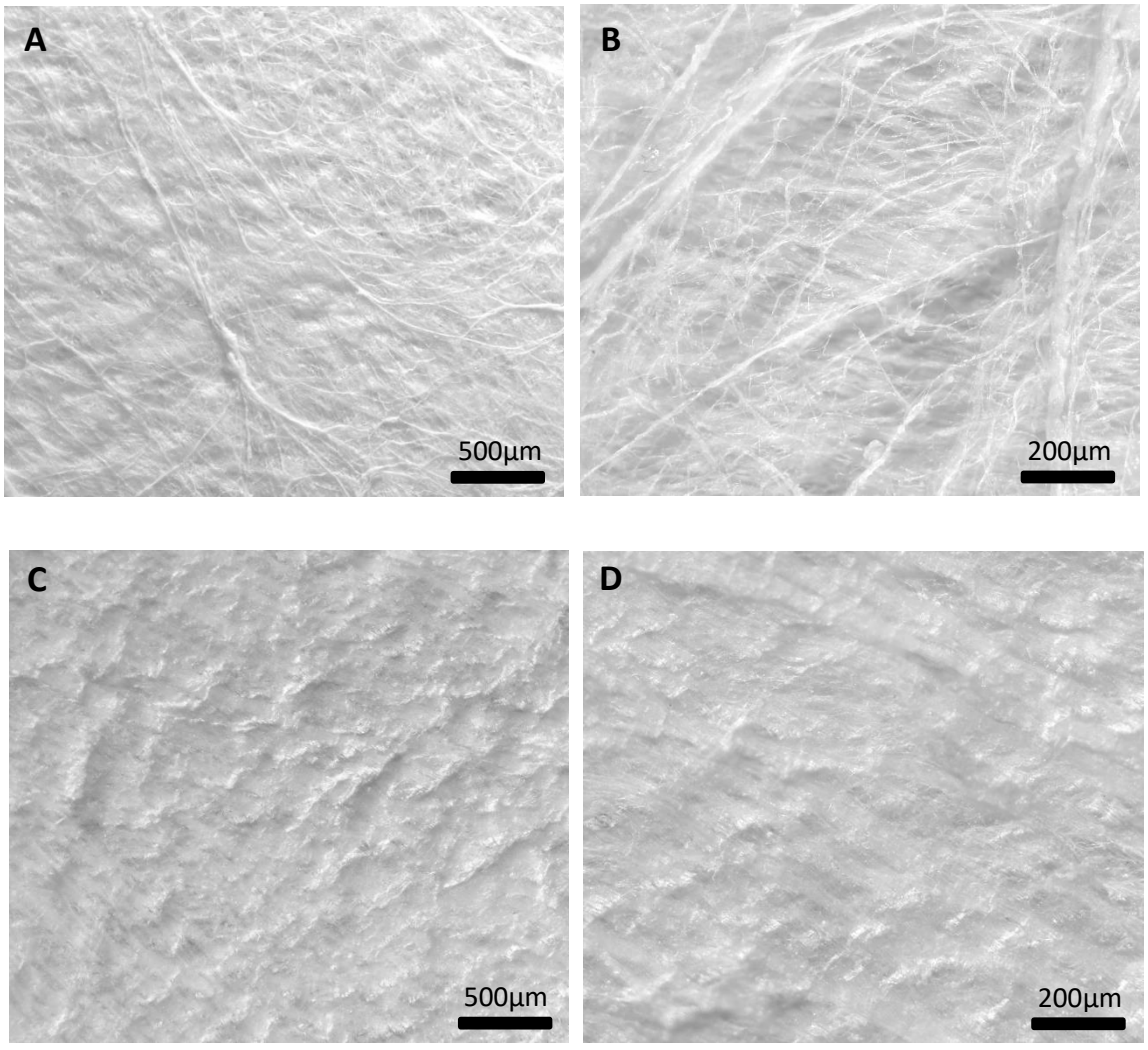

Figure 3: Microscopic view of CelGro membrane
Rough side 40X magnification (A), rough side 100X magnification (B), smooth side 40X magnification (C), smooth side 100X magnification (D)

3.2 CelGro membrane adhesion tensile testing

CelGro's bioadhesive strength was tested on 10 X 30 mm rectangular strips of fresh sheep small intestine placed on a wet cloth for easier manipulation and to minimise sample desiccation. The intestinal strips were cut horizontally together with a cloth backing and 7x5 mm CelGro membrane strips were positioned across the incision on the serosal layer, over the area that was painted with the RB-saline solution (Fig. 4). The membrane was irradiated by a diode pumped solid state 532 nm green laser via an optical fibre (CNI Lasers, China) emitting a beam of 230 mW of power. This power has been previously optimised by Barton et al. (2013) on chitosan-RB films, showing good adhesion with modest tissue heating. The irradiation of the membrane was applied at a distance of approximately 8 mm, producing a beam spot diameter of ~2 mm. The beam was maintained for 5 seconds on each spot before moving to the adjacent spot. The whole surface was scanned three times for a total irradiation time of 200 seconds, producing a fluence of around 131 J/cm^2. Maximum irradiation time for each spot was limited to 5 seconds to avoid excessive heating of the underlying tissue. In our preliminary testing it was found that a wire temperature probe positioned under the CelGro membrane impregnated with the RB-saline solution registered around 10°C temperature increase after 5 seconds irradiation, but this dropped to 6°C when a membrane double layer was used.

Chitosan-RB films of 17±3 μm thickness were prepared following the process described by Lauto et al. (2012) and Barton et al. (2013). This film was attached to cut intestinal strips following the same procedure described above. All intestinal tissue sections were tested 15 minutes after the completion of the repair with a tensiometer (Instron Mini 55, USA). A specimen clamped to the tensiometer grips was separated at a rate of 22 mm/minute until the adhesion failed, and the maximum load was recorded (Fig. 5). Tensile strength was also calculated. I first compared the adhesion strength of lasered smooth and rough sides of CelGro membrane + RB-saline. CelGro membrane + RB-saline adhesion was then compared to the adhesion of CelGro membrane + RB-saline (no lasering), CelGro membrane + saline (lasered) and chitosan-RB film (lasered, Barton et al. 2013).

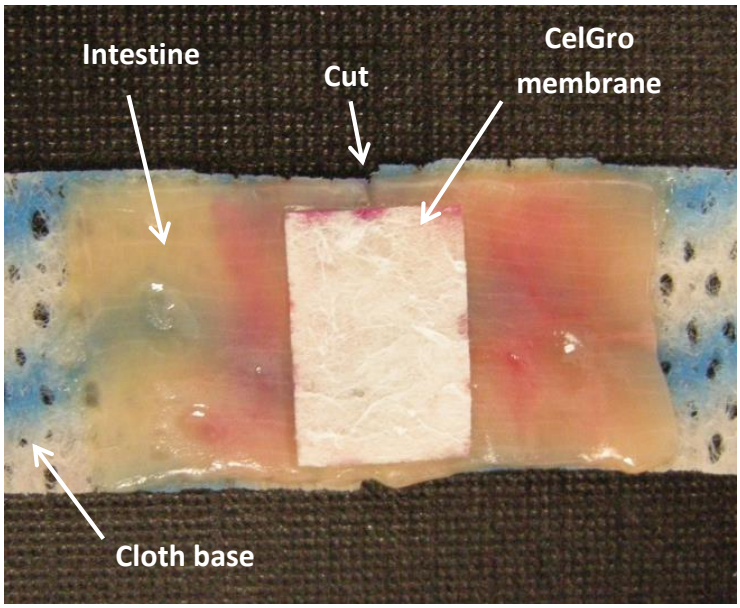

Figure 4: Transected intestine section joined with laser-welded CelGro+RB; section of sheep intestine was placed on a piece of wet cloth (for easier manipulation), with peritoneal surface facing up; both cloth and intestine were cut with scissors, after which the intestinal ends were bonded with laser-activated CelGro+RB membrane

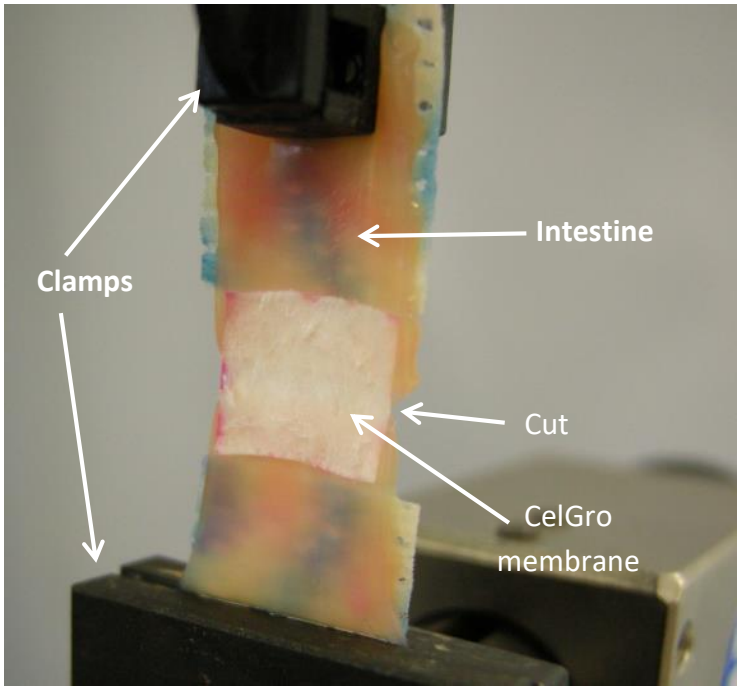

Figure 5: The sample is clamped to the tensiometer using mechanical grips which moved apart until the two tissue stumps separated, at which point the separation force was recorded

3.3. Experimental model

Experimental work on laboratory animals was approved by the Western Sydney University animal care and ethics committee (ACEC: A10622) and all prescribed ethical standards were diligently observed. For all experiments I used 8 week old adult male Wistar rats weighing ~300 g, which, for the duration of the study, were housed in Western Sydney University animal house (School of Medicine, Campbelltown, NSW).

For ***behavioural and electrophysiological work*** 15 animals were randomly allocated into three groups (5 animals in each):

- Sciatic nerve transected and repaired with sutures
- Sciatic nerve transected and repaired with laser-welded CelGro membrane
- CelGro membrane laser-welded around the intact nerve (sham)

For ***histological work*** 30 animals were randomly allocated into the following groups:

- Sciatic nerve transected and repaired with sutures: nerves harvested at 4, 8 and 17 weeks post-surgery (3 animals for each time point)
- Sciatic nerve transected and repaired with laser-welded CelGro membrane: nerves harvested at 4, 8 and 17 weeks post-surgery (3 animals for each time point)
- CelGro membrane laser-welded around the intact nerve: nerves harvested at 4, 8 and 17 weeks post-surgery (sham, 3 animals for each time point)
- Intact nerve with no intervention (control, 3 animals)

3.4 Nerve repair procedure

For all surgical operations general anaesthesia was induced in the induction chamber with 4% isofluorane (VCA, Australia) in 100% oxygen and thereafter maintained with 2.5% isofluorane in 100% oxygen via a nose cone. The rats were placed in prone position and operative site was shaved and prepared with alcohol and povidone iodine as per standard surgical practice. A right side 3 cm skin incision was made with a surgical blade starting 0.5 cm laterally from the animal's midline and extending laterally toward the tibiofemoral joint. Using an Olympus (Japan) operating microscope, the femoral biceps and gluteal muscles were separated by blunt dissection to expose the sciatic nerve which was then mobilised from the surrounding connective tissue. Sciatic nerve transection was performed with surgical micro scissors, at 1 cm above the nerve bifurcation into tibial, fibular and sural nerves (Fig. 6).

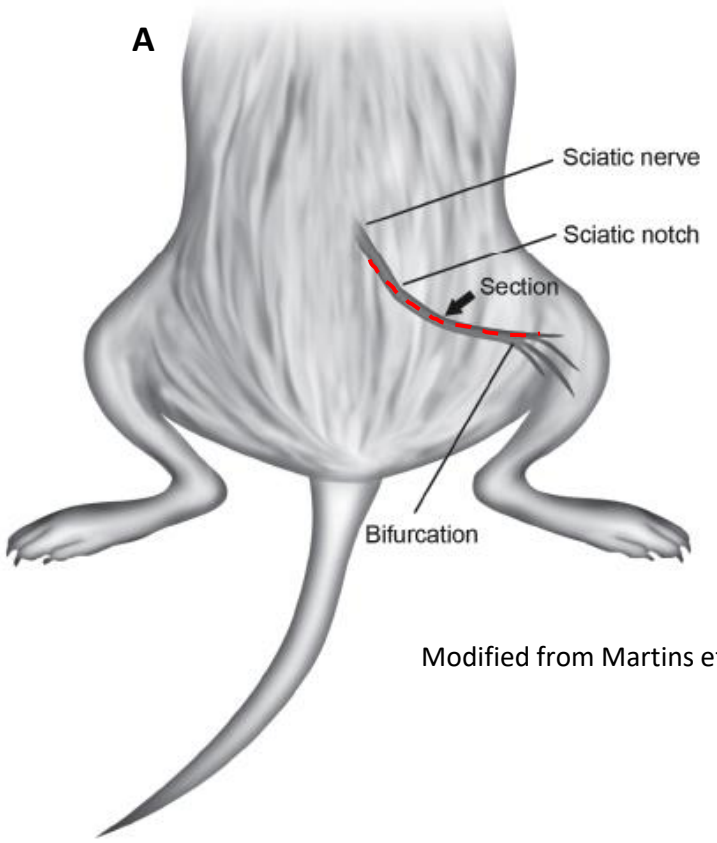

Modified from Martins et al. 2011

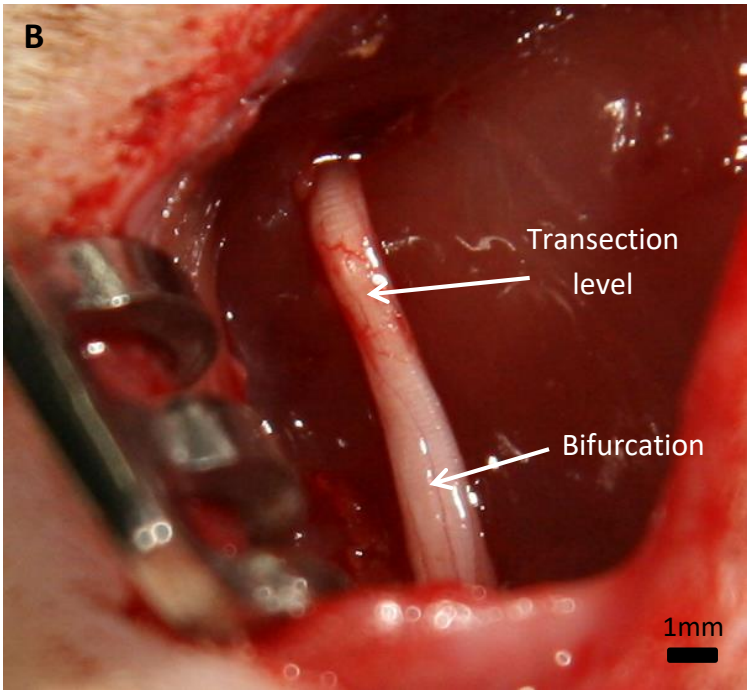

Figure 6: Rat sciatic nerve surgical access

A. Skin incision was done along the dotted red line
B. Exposed sciatic nerve after femoral biceps and gluteal muscles are separated; nerve transection was carried out 1 cm above the anatomical bifurcation

For suture repaired groups, transected nerves were sutured with three epineurial 9-0 nylon monofilaments (Ethilon, Ethicon, USA) by an experienced plastic surgeon as per standard surgical practice on humans (Fig. 7A). Giddins, Wade & Amis (1989) have found 10-0 nylon tends to fail under tension, 9-0 nylon withstood the greater tension force before nerve ends separation, and 8-0 nylon has a tendency to tear the epineurium and pull out of the nerve ending. Care was taken not to pass the suture material deeper than the epineurium and the two nerve ends were gently approximated. The nerves were handled only by using micro forceps, ensuring to grasp the epineurium and not the nerve substance.

For GelGro-repaired groups, CelGro membrane section 6x5 mm was carefully painted with 0.1% RB-saline solution and positioned behind the transected nerve (Fig. 7B). After the approximation and alignment of the nerve ends, the membrane was wrapped around the nerve twice to form a double layered cuff (Fig. 7C). This arrangement reduced the likelihood of thermal damage of the nerve during the laser irradiation and also decreased the possibility of the membrane unwrapping during the recovery period. CelGro membranes were irradiated following the same procedure described in the adhesion tensile testing. This time the entire membrane surface (around 16 mm^2 after double wrapping) was irradiated three times over the 120 second period, producing the fluence of ~172 J/cm^2. It was observed that the CelGro membranes start shrinking after few seconds of laser exposure. In this way on completion of irradiation, the cuff gently and permanently squeezes the nerve ends, which could not be pulled apart even with a moderate force. As the green light wavelength is also absorbed by haemoglobin with some heat generation, I observed a blood clotting effect under the collagen membrane (Fig. 7D). The same described procedure was followed for the sham group that had the CelGro membrane laser-welded around the intact nerve. The entire process is illustrated in Fig. 8. After the nerves were repaired, the separated muscles were brought together with two biodegradable 4-0 suture (Vicryl, Ethicon, USA) and the skin was closed using the stainless steel surgical staples (Autoclip, BD Life Sciences, USA). For postoperative analgesia all operated animals were given buprenorphine 0.05 mg/kg subcutaneously. After the surgery the animals had unlimited access to water and rat chow, and their recovery was regularly checked. Behavioural experiments commenced the following day.

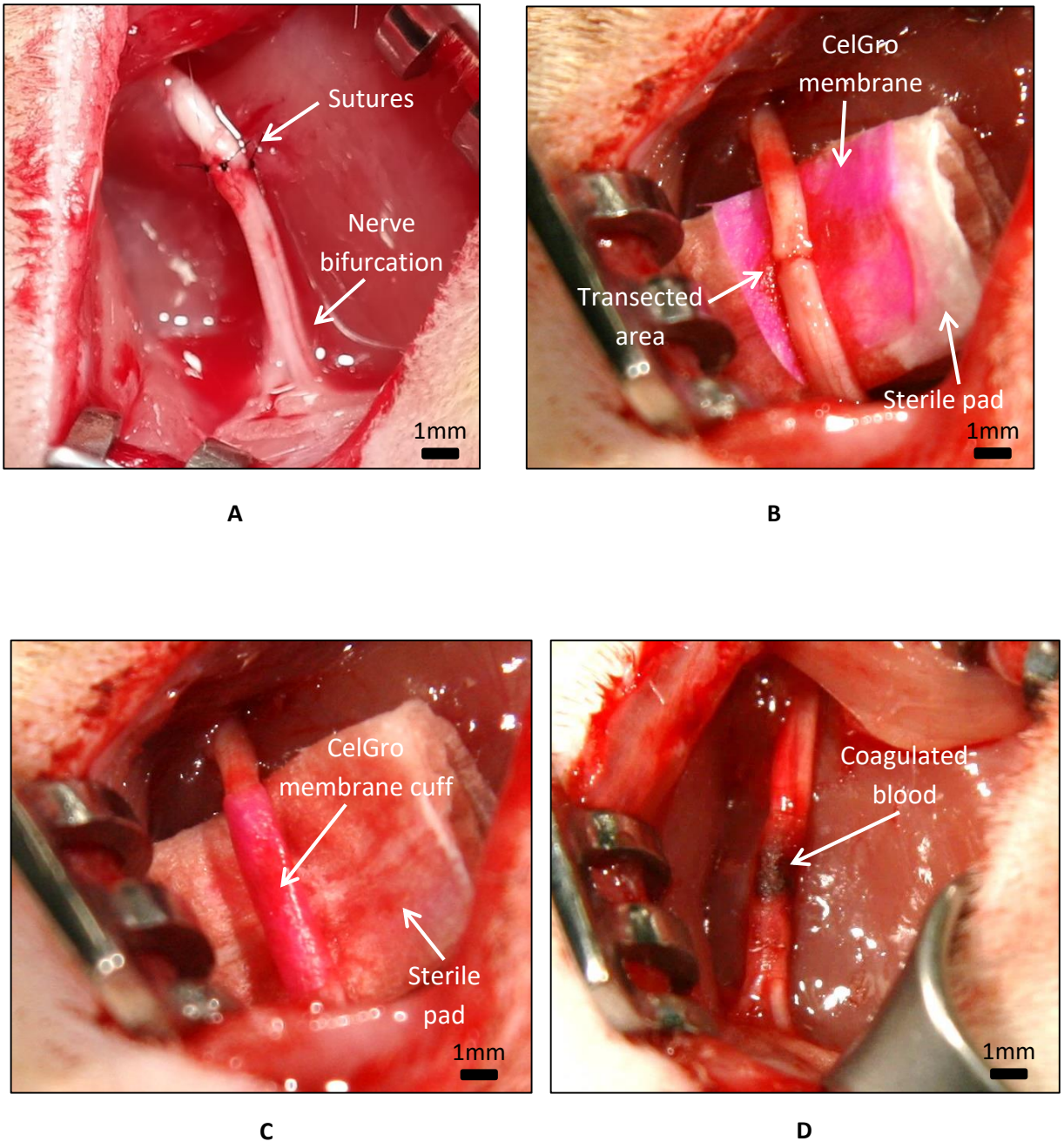

Figure 7: Sciatic nerve repair process

A. Sciatic nerve transected and sutured with three epineurial nylon monofilaments
B. Sciatic nerve transected with CelGro membrane, painted with RB-saline solution, positioned behind the nerve
C. Sciatic nerve wrapped with CelGro+RB membrane forming a double layered cuff, before lasering
D. Sciatic nerve wrapped with a CelGro+RB membrane, after lasering is completed; the cuff shrinks around the nerve; coagulated blood visible under the membrane around the transection area

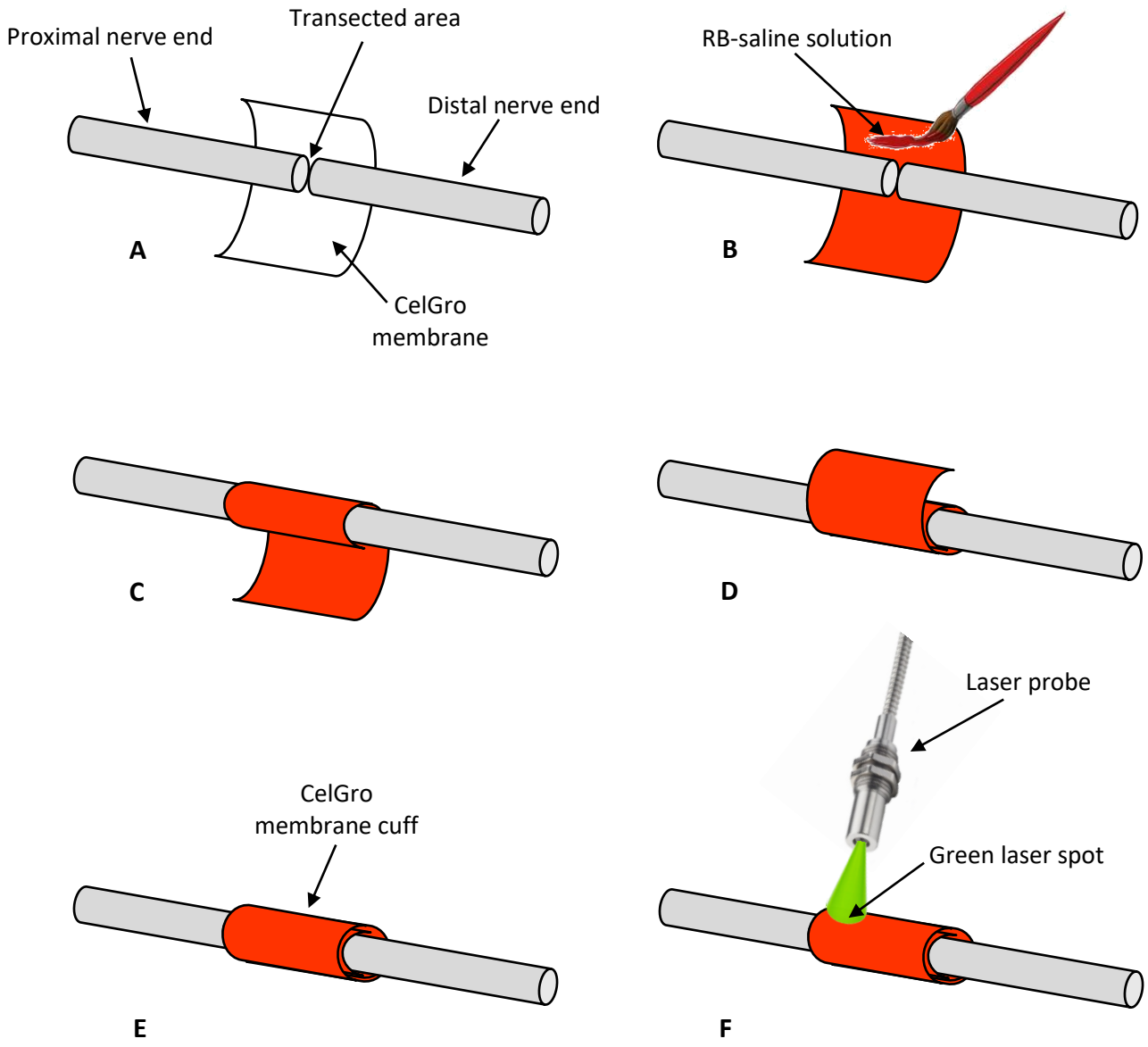

Figure 8: Schematic diagram of CelGro placement and laser-welding procedure

A. Transected nerve ends approximated on top of CelGro membrane
B. CelGro membrane painted with RB-saline solution
C. One end of CelGro wrapped around the coaptation site
D. Other end of CelGro wrapped around the coaptation
E. Double layer CelGro membrane cuff formed
F. Irradiation of membrane with 532 nm green laser

3.5 Behavioural testing for sensory recovery

Two different behavioural tests (withdrawal threshold tests) were performed on three occasions at three day intervals prior to surgery to obtain base-line values. After surgery the testing continued once a week for 17 weeks. On every occasion the animals were left to acclimatise to the testing chamber for 10 minutes before the testing commenced.

- A dynamic plantar Von Frey aesthesiometer machine (Ugo Basile, Italy) was used to deliver *mechanical stimuli* to the plantar surface of the left and right hind paws, avoiding the innervation territory/overlap area of the saphenous nerve, a branch of the femoral nerve (Fig. 9) that could induce a false positive response (De Koning, Brakkee & Gispen 1986). For this testing the rats were placed in plastic boxes on a wire net platform to allow the 0.4 mm diameter needle probe to rise and contact the skin. The machine was set to increase the probe force at 10 g/second until the rat withdrew its paw (time in seconds was measured) or a maximal force of 50 g was reached.

Figure 9: Sensory innervation of the rat hind paw plantar surface (from Cobianchi et al. 2014); mechanical and thermal stimuli delivered to the red area

- *Thermal stimuli* were delivered in a similar fashion through an infrared plantar algesimetry Hargreaves apparatus (Ugo Basile, Italy), utilising infrared intensity of 20 (instrument's unitless scale, adjustable in the interval 01-99). For this test the rats were placed into plastic boxes on a clear plexiglass floor. An infrared beam was delivered through the floor to the hind paw plantar surface, and pointed to the same test site as described above. Latency time (in seconds) for a withdrawal reflex onset

was measured, up until 20 seconds cut off point to prevent tissue injury (Hargreaves et al. 1988, Montagne-clavel & Oliveras 1996, Yeomans & Proudfit 1994).

For both tests on every occasion 5 readings were recorded on both paws (intervention and control) with 1-minute rest interval between the stimuli.

3.6 Electrophysiological testing for motor recovery

Motor recovery was assessed with electromyography measurement of the maximum evoked compound muscle action potential (CMAP) of the gastrocnemius muscle, following the electrical stimulation of the sciatic nerve. The rats were anaesthetised and the sciatic nerves exposed as described earlier. A pair of silver/silver-chloride stimulating electrodes were placed proximal to the repair site on operated nerves. For sham control nerves the electrodes were positioned 1 cm above the nerve bifurcation. The recording electrode was placed on the surface of exposed gastrocnemius muscle making sure to utilise the same location for all groups and both sides. The nerve was stimulated with square electrical impulses (duration 0.2 ms, repetition rate 1 Hz) starting at 10 μA intensity, delivered through the isolated pulse stimulator (A-M Systems, USA). Stimulus intensity was progressively increased until no further increase in muscle response was observed. EMG recordings were captured using the Power1401 analogue to digital converter and Spike2 software (Cambridge Electronic Design, UK), and the maximum amplitude (in mV) was identified.

3.7 Measuring gastrocnemius muscle weight

At the end of electrophysiological data acquisition all animals were sacrificed with a lethal dose of sodium pentobarbital (100 mg/kg) by intraperitoneal injection. Gastrocnemius muscles on both sides were carefully dissected, excised and weighed on an analytical scale (Mettler Toledo ME204, USA) to measure their weight and consequently assess any potential denervation atrophy (Evans et al. 1995).

3.8 Macroscopical nerve analysis and histological studies

For histological studies the animals were first anaesthetised with sodium pentobarbital (60 mg/kg) and then subjected to transcardial whole body perfusion with 250 mL 0.9% saline, followed by 250mL 10% formalin, delivered through a pump set at 60 mL/min flow rate. The

nerves were exposed, photographed in situ, excised in ~8mm length and their widest diameter in the section area measured with a ruler under the operating microscope. The specimens were then placed in 10% formalin for 48 hours and after that the nerves were transferred to 20% sucrose solution for cryoprotection for additional 48 hours, to reduce the water content and minimise ice crystal formation during freezing. The nerves were snap-frozen in OCT medium (Tissue-Tek, Sakura Finetek, USA) in liquid nitrogen and stored in the freezer at -80°C until sectioning on the cryostat. All sections were cut longitudinally in order to visualise the regeneration of axons across the transection line and assess the development of intraneural scarring. Three different types of staining were performed: trichrome, osmium and silver.

3.8.1 Masson's trichrome staining for collagen (Bancroft 2013)

All reagents required for this staining were purchased readymade from Sigma-Aldrich (HT15-1KT, HT1079-1SET and HT10132-1L) and enclosed manufacturer's recommended staining protocol was observed. 12 µm frozen cryostat sections on silane-coated glass slides were oven dried for 8 hours at 50°C and then kept overnight in Bouin's fixative solution. The slides were washed in running water for 15 minutes to remove the yellow colour of picric acid from the sections. The slides were placed in working Iron Haematoxylin solution for 5 minutes and then washed in running water for 5 minutes. The slides were stained with Biebrich Scarlet Acid Fuchsin for 5 minutes and then rinsed in three changes of RO water. The slides were treated on a staining rack with working Phosphotungstic/Phosphomolybdic Acid solution twice (10 minutes each). Phosphoacid solution was then discarded and the slides were stained with Aniline Blue solution for 5 minutes. After rinsing twice in RO water the slides were dehydrated as per standard histological protocol through graded alcohol concentrations (50%, 70%, 95% and 100%), cleared in xylene (two changes), coverslipped with DPX - dibutylphthalate polystyrene xylene (Merck, USA) and examined under light microscope.

3.8.2 Osmium staining for myelin (Miko & Gschmeissner 1994)

Osmium is typically used after glutaraldehyde in specimen preparation for electron microscopy, but can also be employed for direct staining of frozen sections mounted on the glass slide. 16 µm frozen cryostat sections on silane-coated glass slides were oven dried for 8

hours at 50°C and then treated with 1% osmium tetroxide (ProSciTech, Australia) in RO water for 1 hour at room temperature. Osmium tetroxide is a strong oxidant and reacts readily with unsaturated double bonds, which are found in abundance in lipids in myelin sheaths. Oxidation of lipid double bonds causes the reduction of osmium tetroxide with consequent deposition of black osmium dioxide at the site (Kiernan 2007). The intensity of blackening primarily depends on the thickness of the tissue slice. After rinsing three times in RO water for 30 minutes each, the slides were dehydrated through graded alcohol concentrations, cleared in xylene, coverslipped with DPX and examined under light microscope.

3.8.3 Modified Palmgren's silver staining for nerve fibres (Palmgren 1960)

Peripheral nerve axons can be demonstrated with several silver stain protocols in which silver is deposited on cytoskeletal components (neurofilaments) and then reduced to black metallic silver during the development step (Highley & Sullivan 2013). This makes silver staining different from traditional staining protocols, which are essentially a single step procedure and do not involve chemical transformation of the dye. All chemicals for this staining were obtained from Sigma-Aldrich. 14 µm frozen cryostat sections on silane-coated glass slides were oven dried for 8 hours at 50°C and then kept overnight in 20% chloral hydrate solution. The slides were washed three times in RO water for 5 minutes, and then placed in acid formalin (0.002% nitric acid in 10% formalin) for 5 minutes. After washing three times in RO water for 5 minutes, the slides were treated with filtered silver solution (a mix of equal parts of 30% silver nitrate and 20% potassium nitrate, containing 0.05% glycine) for 15 minutes at room temperature. The slides were drained and placed for 1 minute in a reducer solution (1% of pyrogallol in 55% ethanol) that had been heated to 45°C, with continuous gentle rocking to reduce the formation of coarse silver precipitates. The slides were rinsed three times in RO water for 5 minutes, fixed in 5% sodium thiosulfate for 5 minutes and washed again three times in RO water for 5 minutes. After dehydration through graded alcohol concentrations and clearing in xylene, the slides were coverslipped with DPX and examined under light microscope.

3.9 Image acquisition

All gross images were taken with Samsung NX300 camera, and rescaled/cropped in Adobe Photoshop CC.

All microscopic images were taken with Leica DM750 microscope and Leica Application Suite 4.2 software.

3.10 Statistics

All data are presented as mean $\pm$ SD, unless otherwise stated. Data analysis and graphing were carried out using unpaired t-test and 2way ANOVA at a significance level of 0.05 in Prism 6 for Windows (GraphPad Software, USA). Differences between individual samples at the same time points were assessed with a Sidak's multiple comparisons test.

4. Results

4.1 CelGro membrane adhesion testing

Tensile strength characteristics of laser-welded CelGro (smooth side)+RB on sheep intestinal tissue compared to laser-welded CelGro (rough side)+RB are shown in Table 2. When CelGro's rough side was positioned against the tissue, its bonding strength was around 30% less compared to the CelGro's smooth side (significantly inferior). Consequently, I used that side for the remainder of our research.

	Area	Power	Time	Fluence	Maximum load (N)	Tensile strength (kPa)
CelGro (smooth side) + RB	35 mm^2	230 mW	200 sec	~131 J/cm^2	0.36 (0.08)	10.3 (2.3)
CelGro (rough side) + RB	35 mm^2	230 mW	200 sec	~131 J/cm^2	0.25 (0.07)	7.2 (2.6)

Table 2: Laser-welded CelGro+RB adhesion testing comparing its smooth and rough sides facing the tissue surface (n=10, mean ± SD); laser-welded CelGro+RB smooth side is significantly superior to CelGro+RB rough side (unpaired t-test, p = 0.004)

Tensile strength characteristics of laser-welded CelGro+RB on sheep intestinal tissue compared to three controls (CelGro+RB without lasering, laser-welded CelGro+saline without RB, laser-welded chitosan-RB film) are shown in Table 3.

	Area	Power	Time	Fluence	Maximum load (N)	Tensile strength (kPa)
CelGro+RB	35 mm^2	230 mW	200 sec	~131 J/cm^2	0.36 (0.08)	10.3 (2.3)
CelGro+RB (control 1)	35 mm^2	No lasering	NA	NA	0.06 (0.01)	1.7 (0.28)
CelGro+saline (control 2)	35 mm^2	230 mW	200 sec	~131 J/cm^2	0.08 (0.02)	2.3 (0.58)
Chitosan-RB (control 3)	35 mm^2	230 mW	200 sec	~131 J/cm^2	0.44 (0.13)	12.6 (3.7)

Table 3: CelGro+RB adhesion testing compared to controls (n=10, mean ± SD). Laser-welded CelGro+RB is significantly superior to CelGro+RB without lasering (control 1) (unpaired t-test, $p < 0.0001$) and laser-welded CalGro+saline (control 2) (unpaired t-test, $p < 0.0001$); importantly there was no difference between laser-welded CelGro+RB and laser-welded chitosan-RB (control 3) (unpaired t-test, p = 0.11)

CelGro+RB without lasering achieved approximately 16% of the bonding strength of laser-welded CelGro+RB, demonstrating the crucial role of laser irradiation in membrane attachment. Laser-welded CelGro+saline (without RB) achieved only 22% of the bonding strength of laser-welded CelGro+RB, showing a crucial role of RB in membrane attachment. There was no significant difference between laser-welded CelGro+RB and laser-welded chitosan-RB, in regard to the bonding strength.

4.2 Sensory recovery

Wrapping of the intact nerve with CelGro produced a transient hypersensitivity to mechanical and thermal stimuli (Fig. 10, Fig. 11) on the same leg, lasting approximately 3 weeks. Baseline sensation returned from week 4 and remained normal for the duration of the experiment, highlighting absence of long lasting negative effect of the collagen membrane material on sensory processing. There was no detectable change in response to mechanical/thermal stimuli on the healthy leg.

Both CelGro and suture repaired nerves demonstrated initial anaesthesia, that improved 4 weeks post-surgery, and reached baseline levels by week 6, after which both became hypersensitive, peaking around week 8 post-surgery. From that point, the hypersensitivity slowly resolved and met baseline at week 14 (for thermal withdrawal, CelGro repair, Fig. 12), week 15 (for mechanical withdrawal, CelGro repair, Fig. 15) and week 17 (for thermal and mechanical withdrawal, suture repair, Fig. 13 and Fig. 16) post-surgery. Compared to suture repaired nerves, CelGro demonstrated significantly better sensory recovery from anaesthesia, less hyperaesthesia and 2-3 weeks earlier return to the baseline (Fig. 14 and Fig. 17). However, both types of nerve repair showed similar sensory recovery results at the very end of the experiment (week 17).

4.3 Motor recovery

EMG compound muscle action potential of gastrocnemius muscles and their weight showed no significant difference between the CelGro wrapped nerves and the contralateral side, therefore demonstrating no negative impact of the membrane on motor nerve activity and its respective muscle innervation (Fig. 18 and Fig. 19).

Both CelGro and suture repaired nerves demonstrated a significant decrease of the gastrocnemius compound muscle action potential and gastrocnemius muscle weight compared to their corresponding opposite side controls (Fig. 18 and Fig. 19). The CMAP amplitude is proportional to the number of regenerated motor axons and the size of the corresponding motor units (all muscle fibres innervated by a single motor axon) in the tested muscle (Navarro & Udina 2009). This result shows that the muscle activity has not returned to normal at the end of the experiment (17 weeks).

However, CelGro repaired nerves demonstrated significantly greater gastrocnemius muscle CMAP and weight compared to suture repaired nerves (Fig. 18 and Fig. 19), suggesting a superior motor recovery and functional re-innervation.

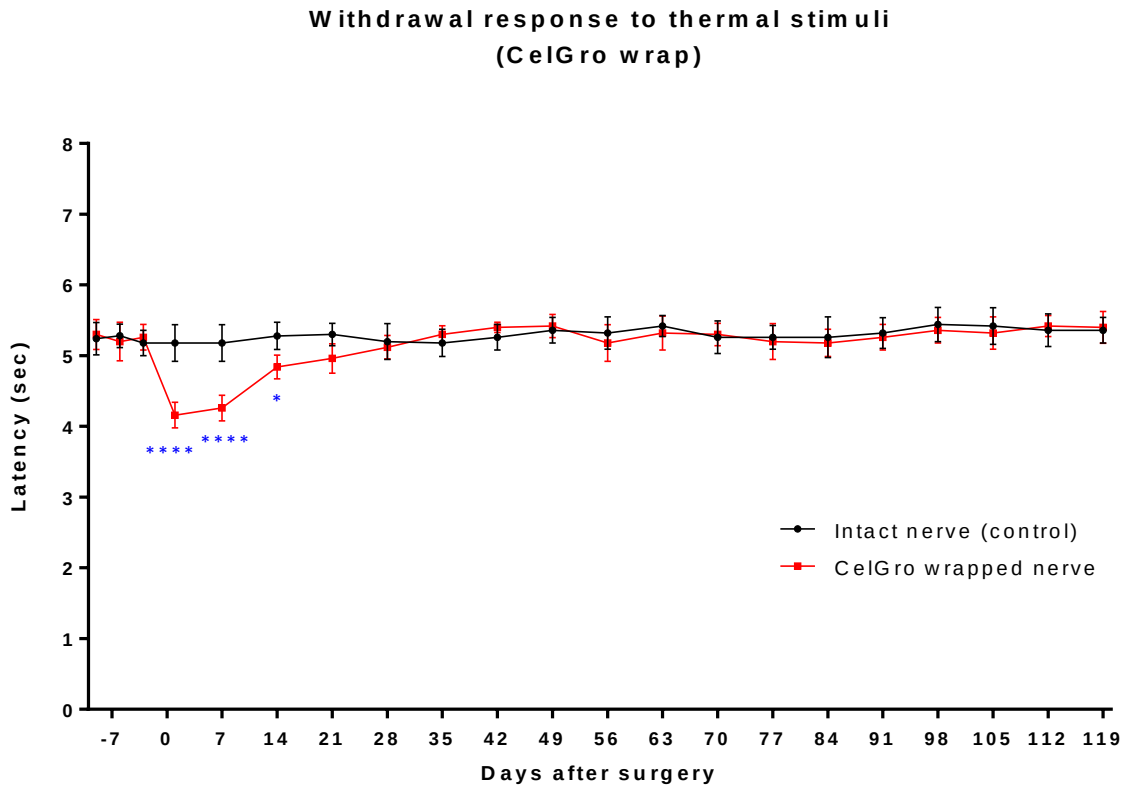

Figure 10: Thermal withdrawal testing of CelGro wrapped healthy nerves versus the contralateral healthy intact nerves; significant hyperaesthesia on the wrapped side from day 1 post-surgery (2way ANOVA, * = $p \leq 0.05$, **** = $p \leq 0.0001$, non-labelled time points not significantly different, n=5, mean ± SD)

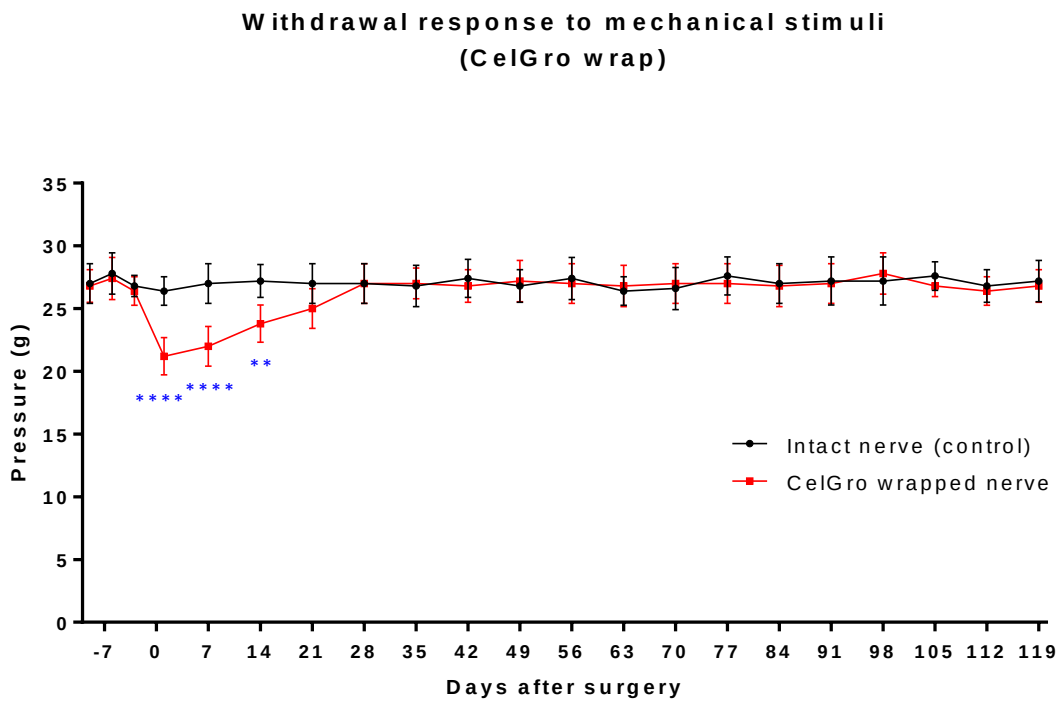

Figure 11: Mechanical withdrawal testing of CelGro wrapped healthy nerves versus the contralateral healthy intact nerves; significant hyperaesthesia on the wrapped side from day 1 post-surgery (2way ANOVA, ** = $p \leq 0.01$, **** = $p \leq 0.0001$, non-labelled time points not significantly different, n=5, mean ± SD)

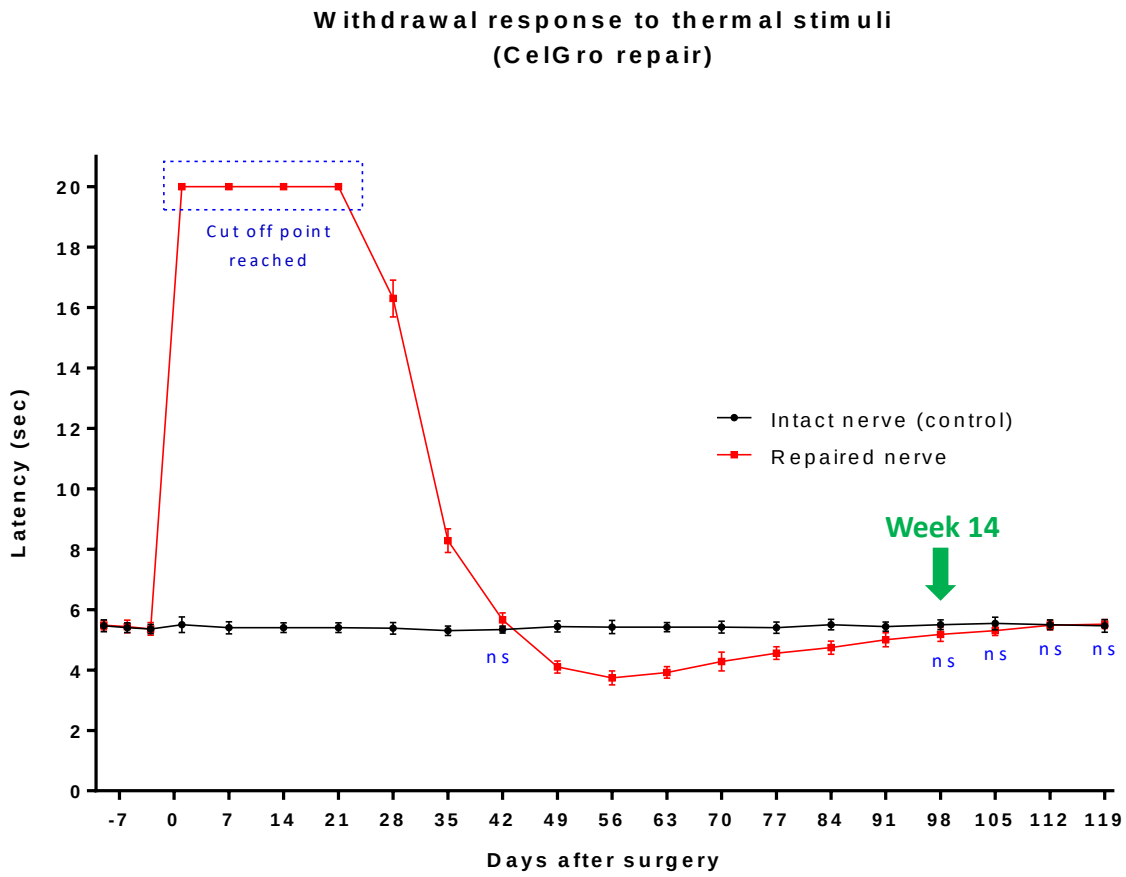

Figure 12: Thermal withdrawal testing of CelGro repaired nerves versus the contralateral healthy nerves; initial anaesthesia, followed by recovery and hyperaesthesia returning to normal effectively at week 14 (2way ANOVA, ns = not significant, non-labelled time points after surgery are significantly different, n=5, mean ± SD)

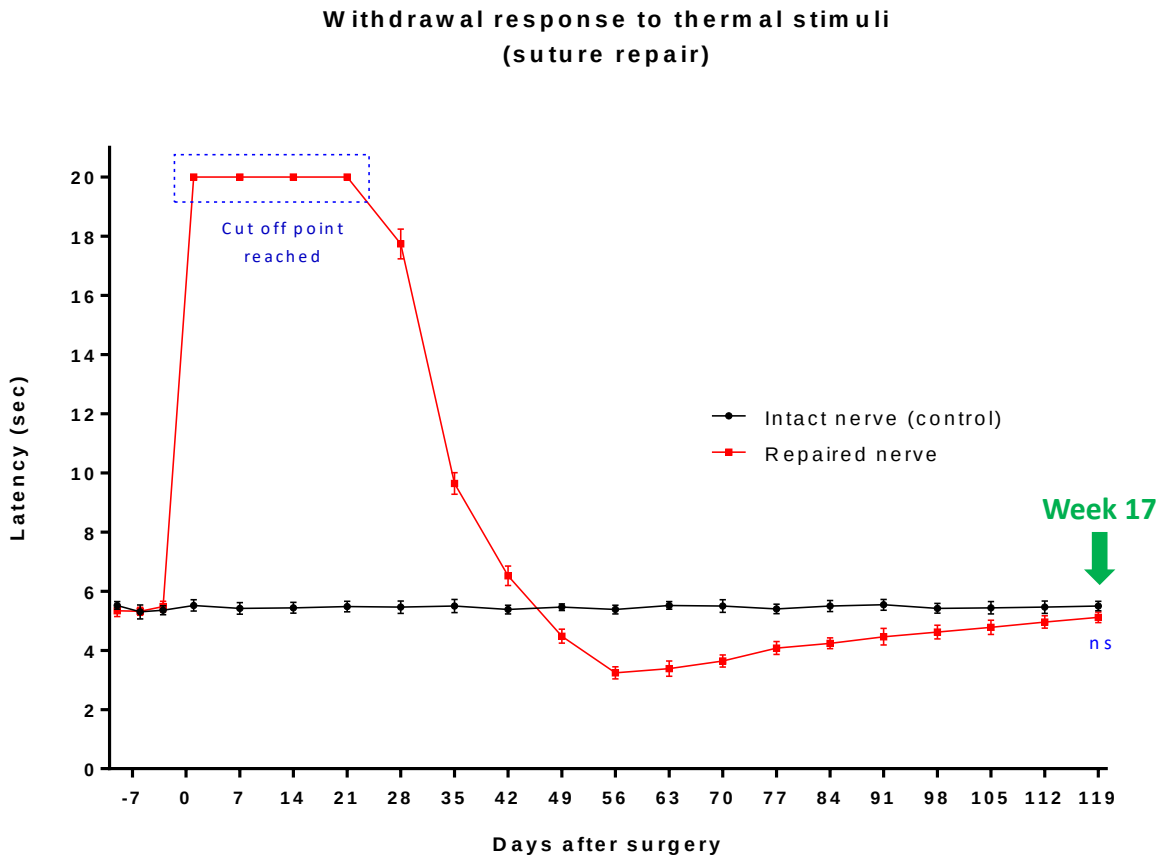

Figure 13: Thermal withdrawal testing of suture repaired nerves versus the contralateral healthy nerves; initial anaesthesia, followed by recovery and hyperaesthesia returning to normal at week 17 (2way ANOVA, ns = not significant, non-labelled time points after surgery are significantly different, n=5, mean ± SD)

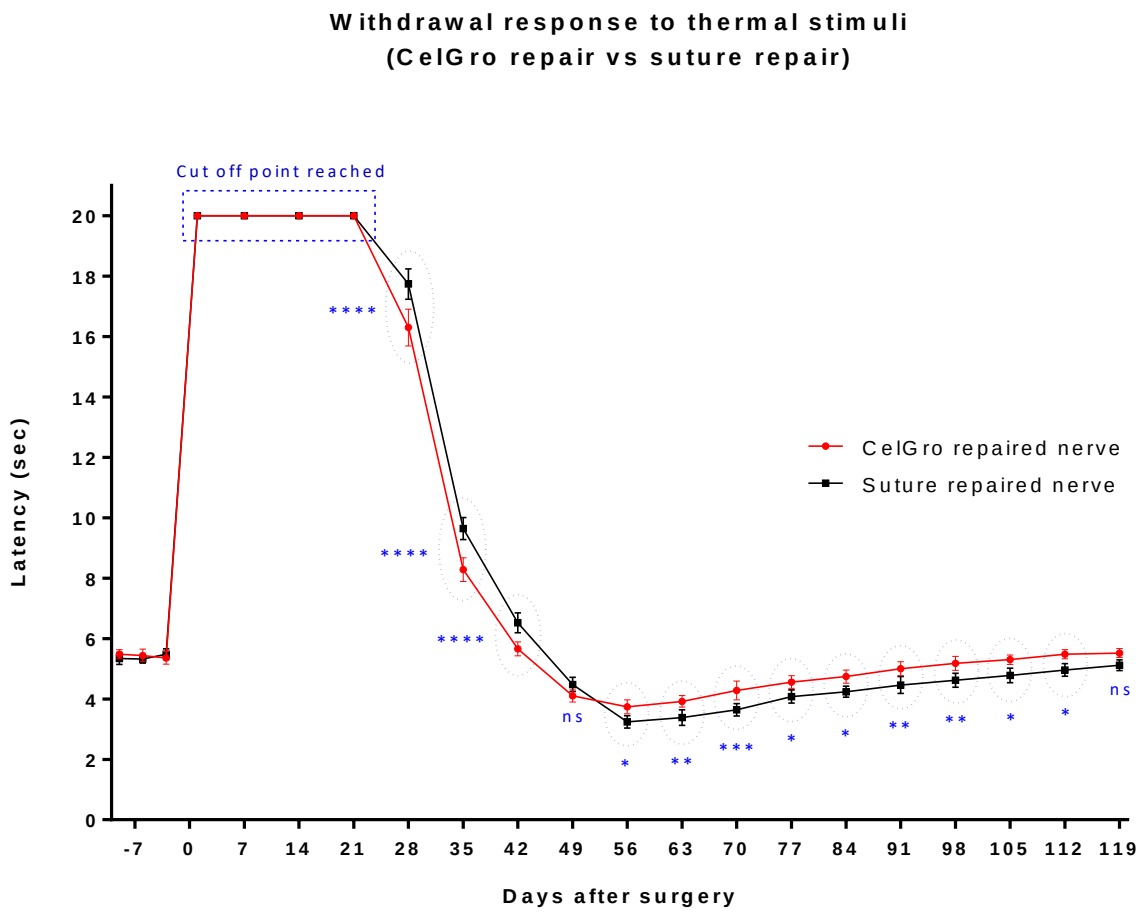

Figure 14: Thermal withdrawal testing comparison of CelGro and suture repaired nerves; CelGro repaired nerves show significantly better recovery from initial anaesthesia, reach less hyperaesthesia and show faster recovery from hyperaesthesia (2way ANOVA, * = $p \leq 0.05$, ** = $p \leq 0.01$, *** = $p \leq 0.001$, **** = $p \leq 0.0001$, , ns = not significant, n=5, mean $\pm$ SD)

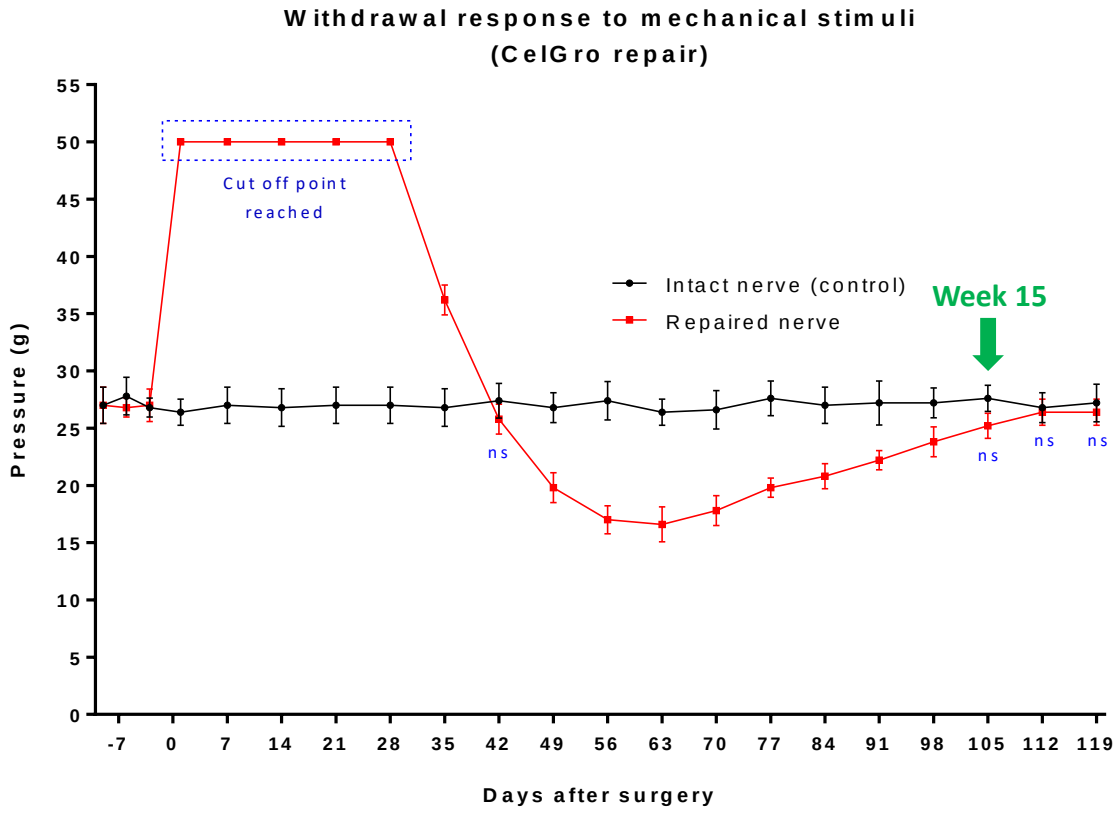

Figure 15: Mechanical withdrawal testing of CelGro repaired nerves versus the contralateral side; initial anaesthesia, followed by recovery and hyperaesthesia returning to normal processing effectively at week 15 (2way ANOVA, ns = not significant, non-labelled time points after surgery are significantly different, n=5, mean ± SD)

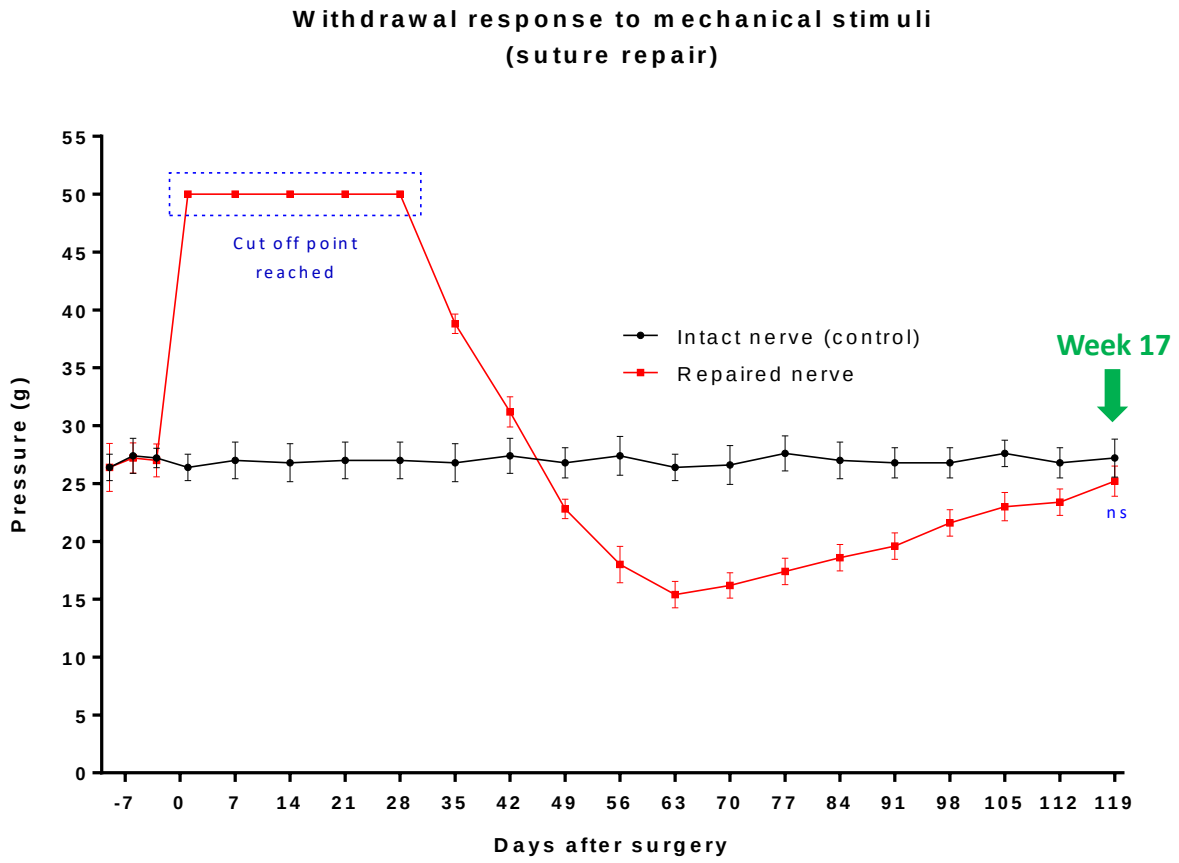

Figure 16: Mechanical withdrawal testing of suture repaired nerves versus the contralateral side; initial anaesthesia, followed by recovery and hyperaesthesia returning to normal processing at week 17 (2way ANOVA, ns = not significant, non-labelled time points after surgery are significantly different, n=5, mean ± SD)

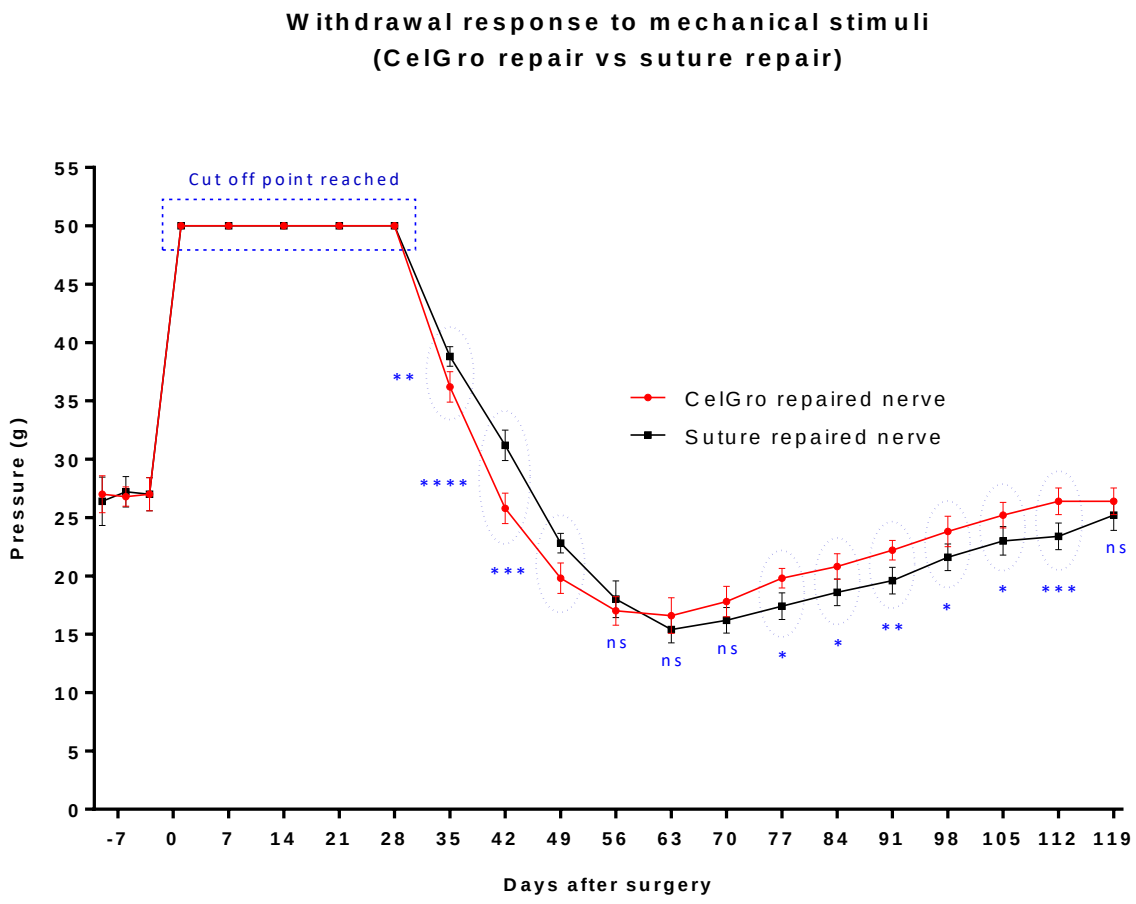

Figure 17: Mechanical withdrawal testing comparison of CelGro and suture repaired nerves; CelGro repaired nerves show significantly better recovery from initial anaesthesia, reach less hyperaesthesia and show faster recovery from hyperaesthesia (2way ANOVA, * = $p \leq 0.05$, ** = $p \leq 0.01$, *** = $p \leq 0.001$, **** = $p \leq 0.0001$, , ns = not significant, n=5, mean ± SD)

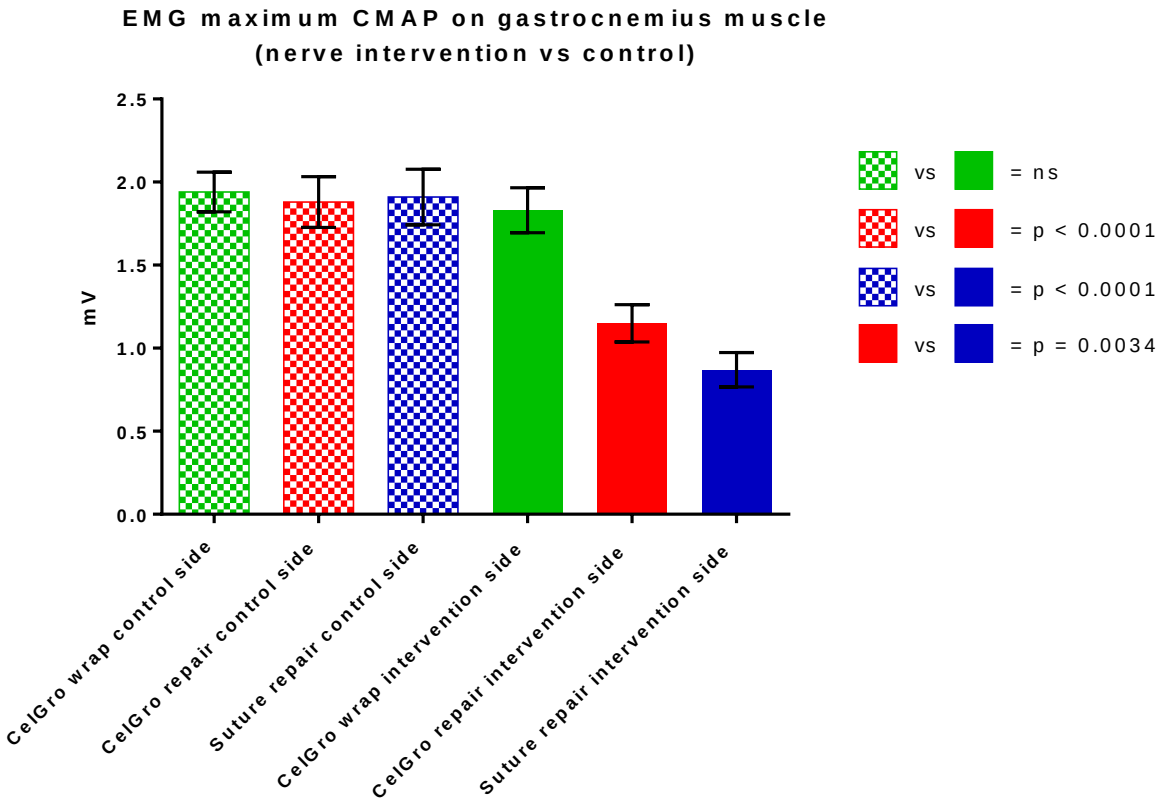

Figure 18: Maximum compound muscle action potential on gastrocnemius muscles that was produced in three experimental groups at the end of experiment (17 weeks post-surgery); contralateral muscles in each group were used as controls; CelGro wrapping around intact nerves did not affect the electrophysiological response; neither CelGro repaired nor suture repaired nerves returned their electrophysiological response to normal levels; CelGro repaired nerves show significantly greater CMAP than suture repaired nerves (unpaired t test, n=5, mean ± SD)

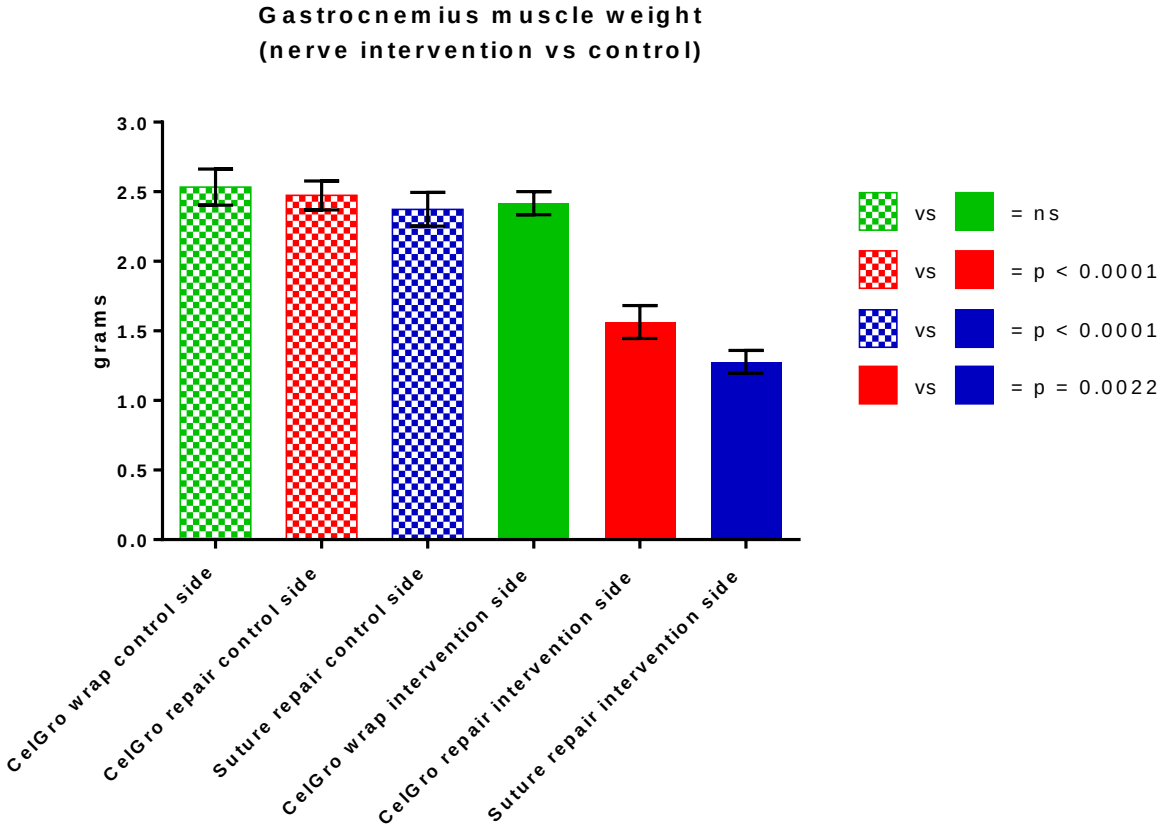

Figure 19: Weight of gastrocnemius muscles measured in three experimental groups at the end of experiment (17 weeks post-surgery); contralateral muscle in each group served as a control; CelGro wrapping around intact nerve did not affect the muscle weight; neither CelGro repaired nor suture repaired nerves returned their gastrocnemius weight to normal levels; CelGro repaired nerves show significantly larger muscle weight (63% of the control) than suture repaired nerves (52% of the control) (unpaired t test, n=5, mean ± SD)

4.4 Nerve macroscopy analysis

All repaired nerves (27 in total, in 3 groups) were visually inspected macroscopically during specimen harvesting for histology at 4 weeks, 8 weeks and 17 weeks post-surgery (Fig. 20) and compared to intact nerves (control group, 3 nerves). The results in different animals in the same group were found to be consistent.

- CelGro membrane wrapped around the intact nerves was still evident at 4 week, after which it started desintegrating, appearinjg largely degraded by week 8, and disappeared by week 17. No fibrous adhesions with the sourounding tissue were observed and the nerves were easily mobilised.
- CelGro membrane wraps around the transected nerves managed to produce and maintain excellent alignment of the nerve stumps throughout the observation period. I did not experience any bond failure. The membrane showed almost identical biodegradability dynamics. It was barely there at 8 weeks, while no traces could be seen at 17 weeks. At this point the repaired nerves demonstrated virtually normal anatomical appearance. Additionally, there were no visible adhesions between the repaired nerves and the surounding muscle/connective tissue.
- In contrast, sutured nerves showed visible deformities in form of swelling, in the suture region, at all three time points. Even though anatomical appearance of the sutured nerves improved with time, the swellings still persisted at week 17 and are likely to be permanent. These observed deformites appear to be caused by compression-induced misalignment of approximated nerve ends, disorganised axonal growth and development of intraneural scarring, as evidenced on microscopy of histological samples. Furthermore, fibrous adhesions with the surounding tissues were observed around all sutured nerves. These adhesions had to be carefully cut in order to harvest the nerves for histology.

At the end of the experiment (17 weeks), there was no statistical difference between the transection line thickness of CelGro wrapped nerves, CelGro repaired nerves and the control intact nerves. That showed effective biodegradability of the CelGro membrane, as well as good restoration of anatomcal structure of the CelGro repaired nerves. Sutured nerves, on the other hand, were significantly thicker (~12%) around the transection line than the control

nerves as well as CelGro repaired nerves, demonstrating their suboptimal anatomical recovery (Fig. 21). This appearance is in line with development of neuroma-in-continuity composed of a mixture of aberrant, tangled axonal rengeneration and intraneural connective tissue (Alant et al. 2012).

	4 weeks	8 weeks	17 weeks
CelGro wrap	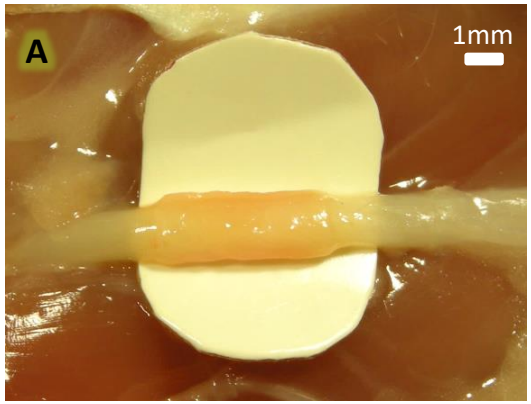	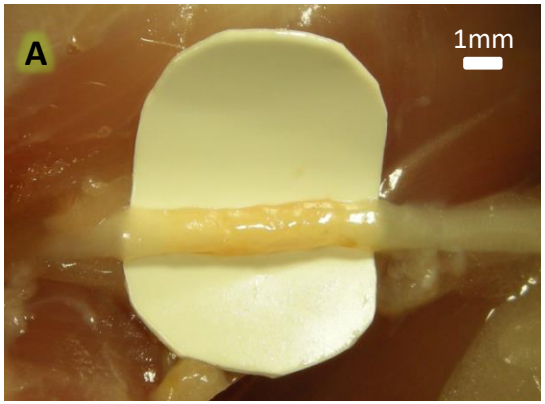	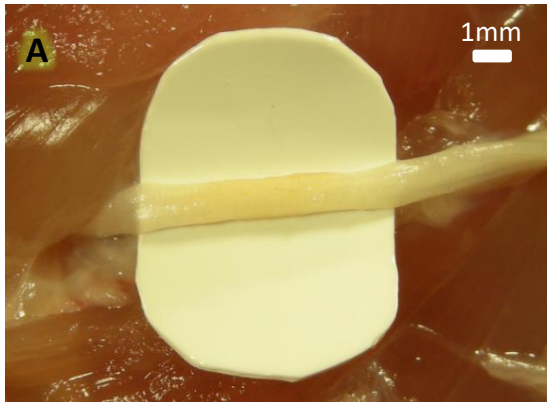
CelGro repair	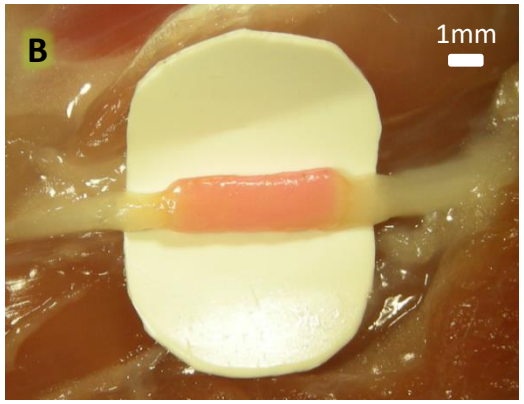	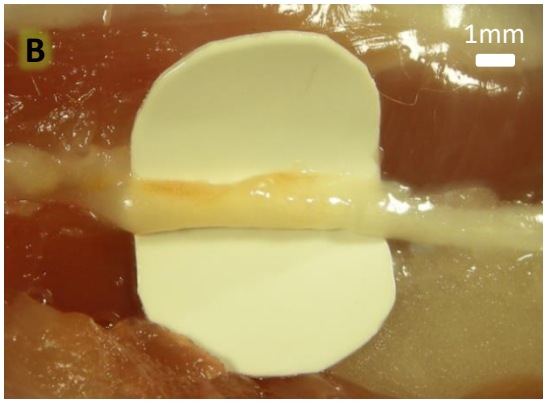	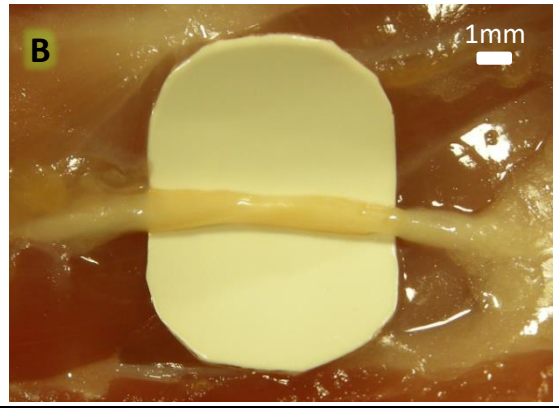
Suture repair	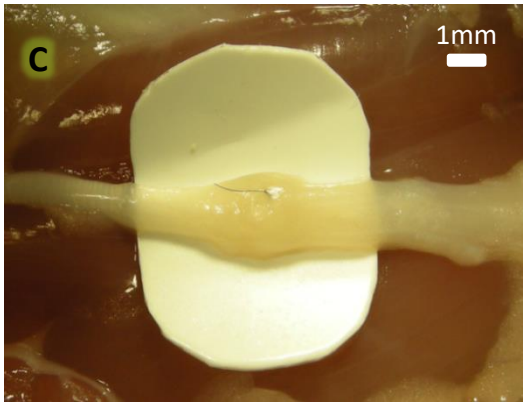	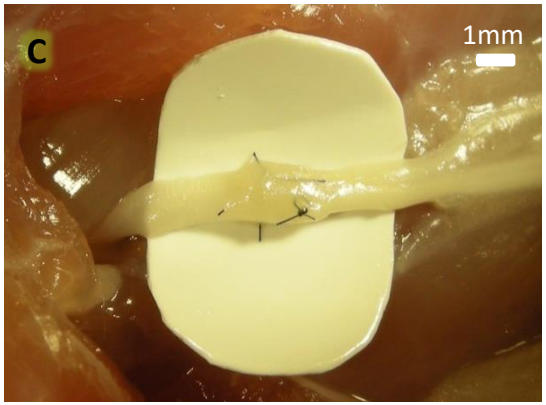	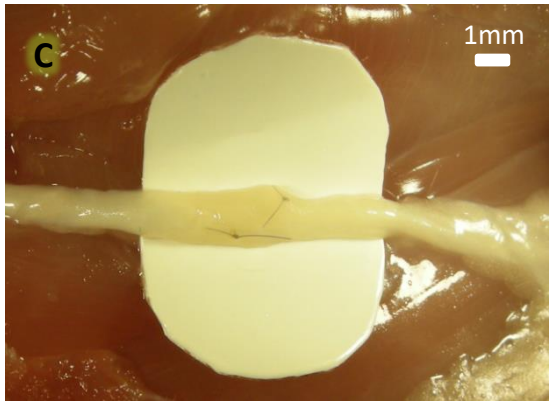

Figure 20: Macroscopic appearance of nerves post- surgery, before nerve harvesting

- 4 weeks post-surgery
  A. CelGro wrap around intact nerve; membrane cuff clearly seen projecting above the nerve surface, RB colour almost faded away
  B. CelGro repair of cut nerve, membrane cuff projects above the nerve surface , keeps cut ends well aligned, RB colour only partially bleached
  C. Suture repair of cut nerve; black sutures visible, nerve swelling prominent, caused by compression of nerve ends together by tension of placed sutures

- 8 weeks post-surgery
  A. CelGro wrap around intact nerve; membrane largely dissolved, barely projecting above the nerve surface, RB colour faded away
  B. CelGro repair of cut nerve, membrane partially dissolved, alignment preserved, , barely projecting above the nerve surface, RB colour faded away
  C. Suture repair of cut nerve; permanent sutures visible, nerve swelling still persists

- 17 weeks post-surgery
  A. CelGro wrap around intact nerve; membrane completely dissolved, no trace of RB colour, appearance largely normal
  B. CelGro repair of cut nerve, membrane almost completely dissolved, no trace of RB colour, regenerated nerve subjectively appears somewhat thinner around the transection line
  C. Suture repair of cut nerve; permanent sutures clearly visible, nerve swelling subjectively less evident than after 8 weeks but still apparent, consistent with development of neuroma-in-continuity

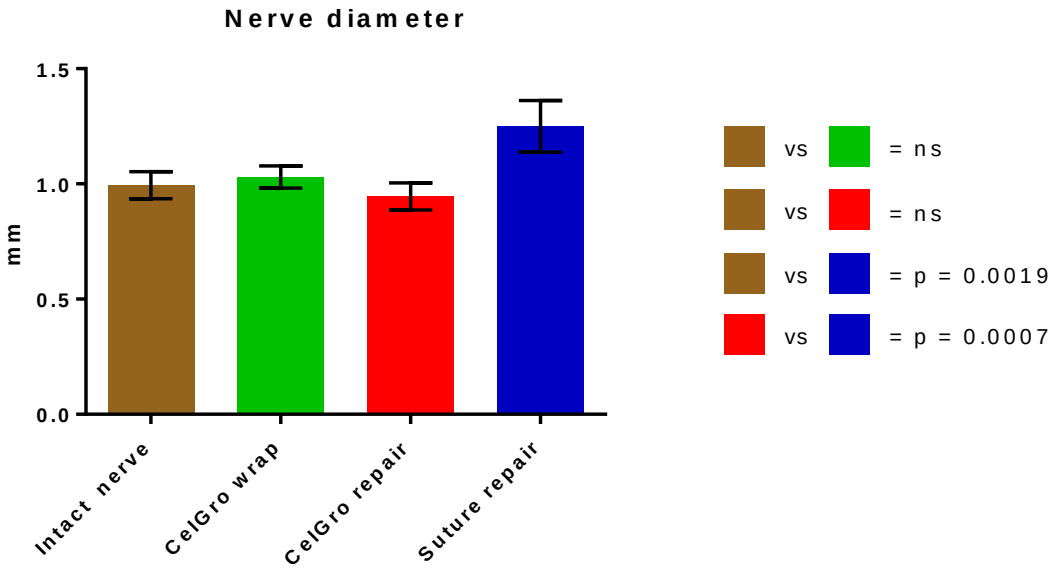

Figure 21: Nerve diameter measured around the transection line in three experimental groups at the end of experiment (17 weeks post- surgery); there was no significant difference between the intact nerves and CelGro wrapped nerves, or between the intact nerves and CelGro repaired nerves; significant difference was found when comparing the intact nerves and suture repaired nerves, as well as CelGro repaired nerves and suture repaired nerves (unpaired t test, n=3 for each experimental group, mean ± SD)

4.5 Nerve histological analysis

All repaired nerves (27 in total, in 3 groups) were harvested and prepared for histology at 4 weeks, 8 weeks and 17 weeks post-surgery (3 animals for each time point), and compared histologically with the intact control nerves (3 animals, Fig. 22).

- Intact nerves wrapped with CelGro did not show obvious evidence of intraneural inflammatory response (indicated by lack of hypercellularity within the nerve) and axons' histology was essentially normal. CelGro membrane material showed good degradability, slowly becoming fragmented and integrated into the epineurium connective tissue (Fig. 23, Fig. 26, Fig. 29). The membrane material was virtually dissolved by week 8, and no remnants were visible by week 17. Small number of cells was observed within the membrane material throughout this process, consistent with infiltration by the inflammatory cells and fibroblasts. After 17 weeks, there was no histological difference from the control nerves, with the epineurium regaining its normal structure and thickness.
- CelGro repaired nerves maintained good alignment of the coapted stumps and in time the membrane slowly degraded becoming an integral part of the epineurium. There was also modest infiltration of the membrane material with the cells, likely to be macrophages and fibroblasts. More vigorous cellular response, together with fragmentation of distal axonal segments, was observed around and below the transection line at week 4 post-surgery, corresponding with the macrophages and Schwann cells activity. This intraneural cellular response was largely subsided by week 8 and absent by week 17. Axon regeneration/myelination showed good progress and by week 17 post-surgery the nerve was largely normal in histological appearance (Fig. 24, Fig. 27, Fig. 30). There was no presence of the residual membrane material around the nerve at this point, and the epineurium showed structural features comparable to intact nerves.
- Sutured nerves showed suboptimal alignment of the coapted ends with a marked thickening in the transection area. This swelling was observed at all 3 time points. Inflammatory cellular response was very marked at week 4 around and below the transection area, in line with Wallerian degeneration of severed axons. This hypercellularity got less intense in time but was still present at both weeks 8 and 17,

suggesting an ongoing inflammatory reaction. There was disordered histological architecture of the fascicles with numerous axons misdirected and not getting across the transection line, or being forced to detour to avoid the sutures that got deeply embedded in the nerve (Fig. 25, Fig. 28, Fig. 31). Substantial scarring within the nerve was identified in all time points and was of a particular concern in regard to its ability to act as an effective barrier against axon growth. Such appearance is consistent with a neuroma-in-continuity, which refers to a mass of tangled, usually poorly myelinated or unmyelinated axons, connective tissue and cells such as Schwann cells, macrophages and fibroblasts. This development is more marked in poor fascicular realignment when many regenerating axons penetrate into interfascicular tissue, where they grow and branch in a disorganised way (Mavrogenis et al. 2008).

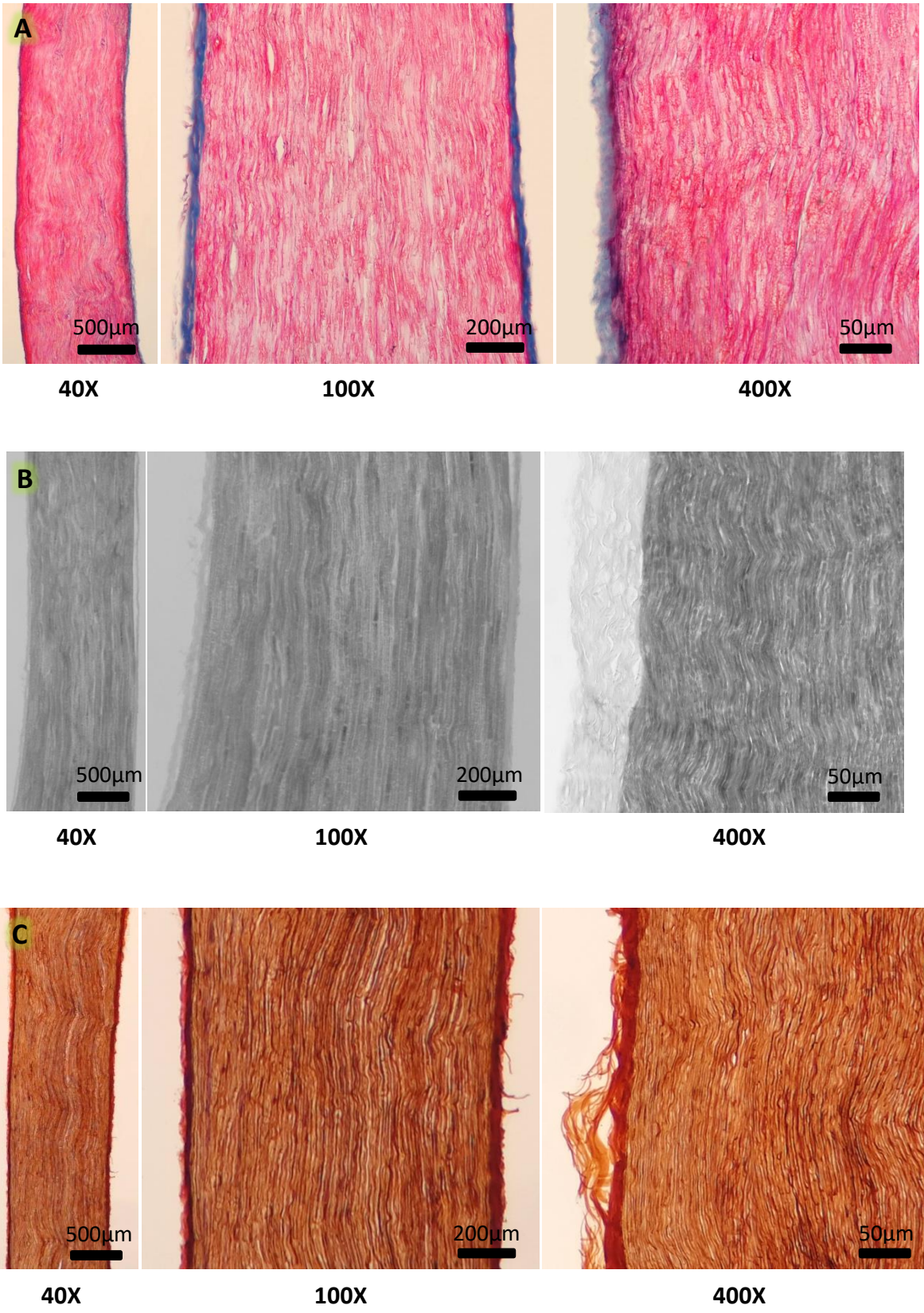

Figure 22: Normal nerve (control) histology, longitudinal section

A. Masson's trichrome stain (axons red, connective tissue blue)
B. Osmium stain (myelinated axons dark grey, connective tissue light grey)
C. Silver stain (axons dark brown/black, connective tissue light brown)

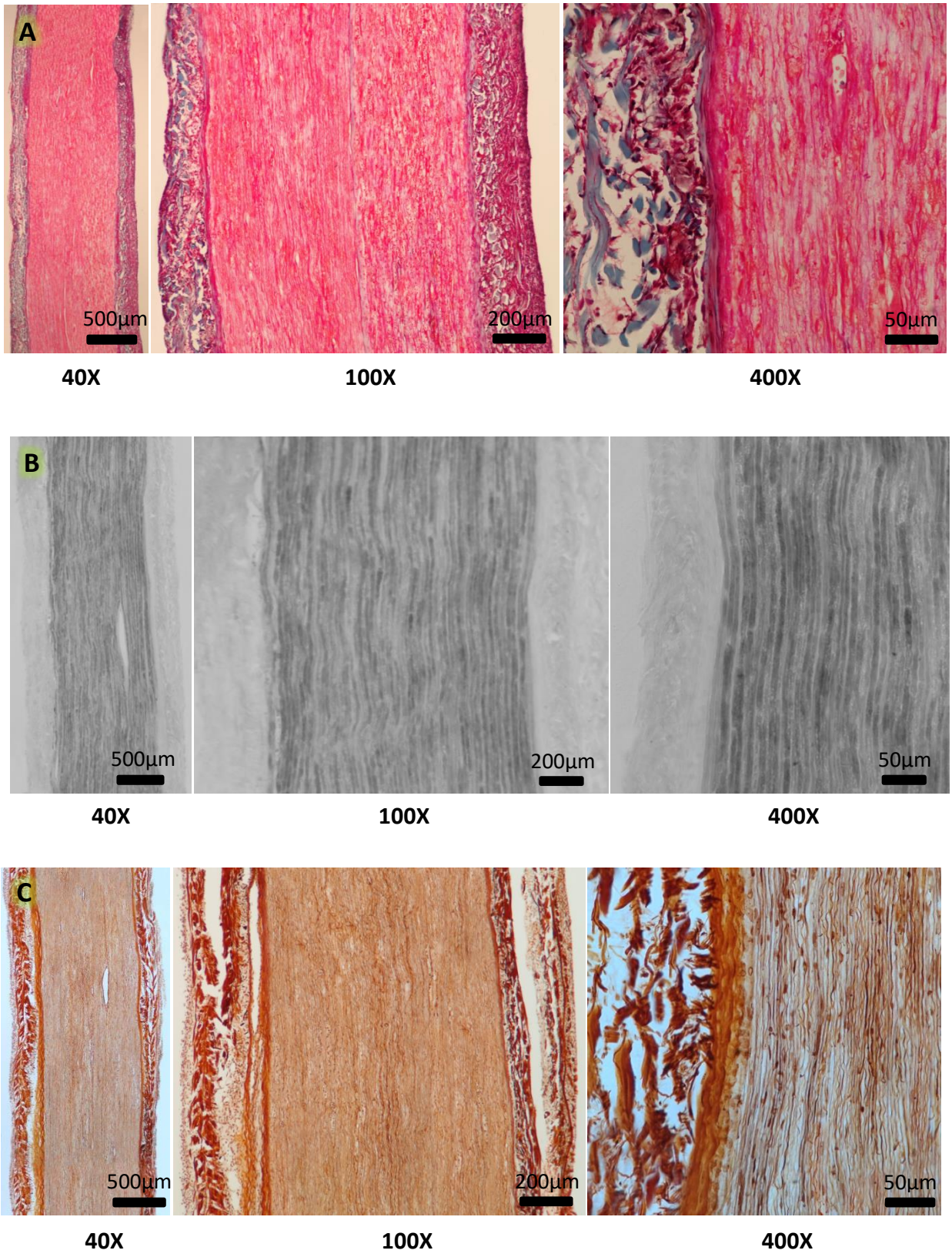

Figure 23: CelGro wrap 4 weeks post-surgery histology, longitudinal section

A. Masson's trichrome stain (normal nerve histology, no apparent hypercellularity within nerve, membrane material already disintegrating)
B. Osmium stain (normal nerve histology, myelinated axons preserved, faint membrane material around nerve)
C. Silver stain (normal nerve histology, preserved axon threads continuity, disintegrating membrane material)

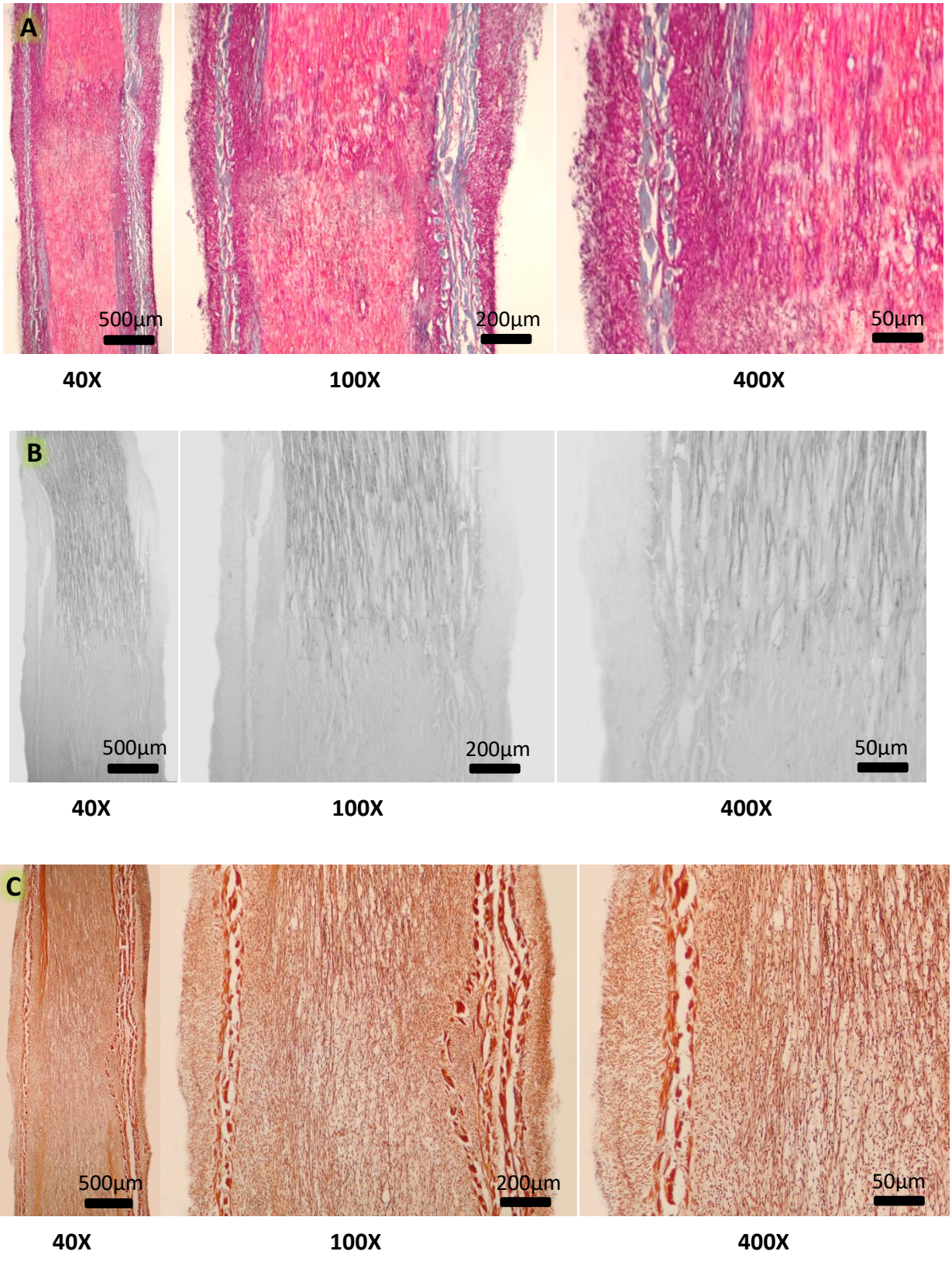

Figure 24: CelGro repair 4 weeks post-surgery histology, longitudinal section

A. Masson's trichrome stain (axon continuity disrupted, increased cellularity in section area, nerve alignment preserved by membrane cuff)
B. Osmium stain (myelinated axon continuity disrupted, nerve alignment preserved by membrane cuff, axon budding)
C. Silver stain (myelinated axon continuity disrupted, increased cellularity in section area, axon budding apparent, nerve alignment preserved by membrane cuff)

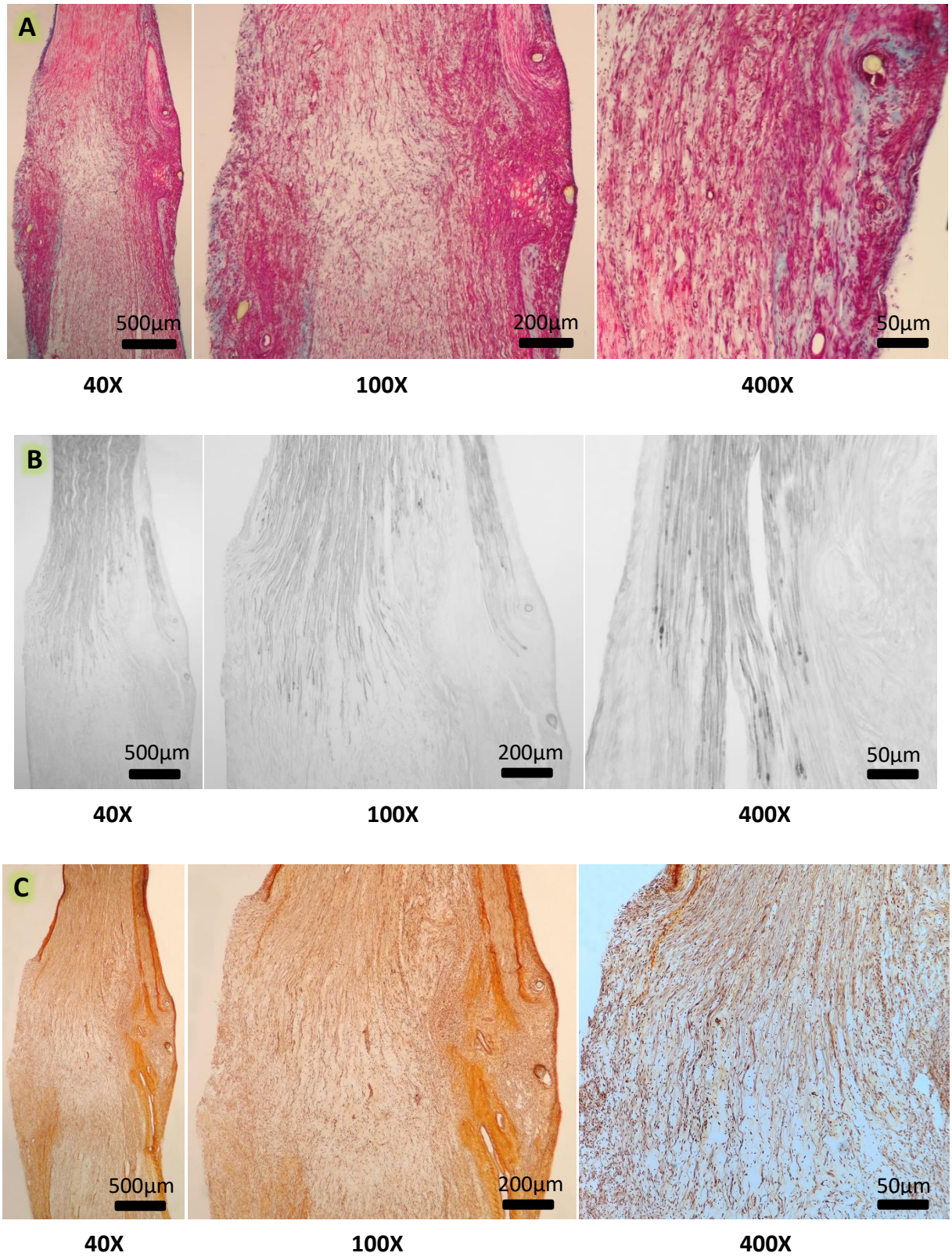

Figure 25: Suture repair 4 weeks post-surgery, histology longitudinal section

A. Masson's trichrome stain (disruption of architecture, axon continuity disrupted, increased cellularity in the section area, substantial fibrosis within the nerve, especially around sutures)
B. Osmium stain (substantial nerve swelling, disruption of myelinated axon continuity, axon budding in uneven fashion)
C. Silver stain (substantial nerve swelling, connective tissue deposition within nerve, disruption of axon continuity)

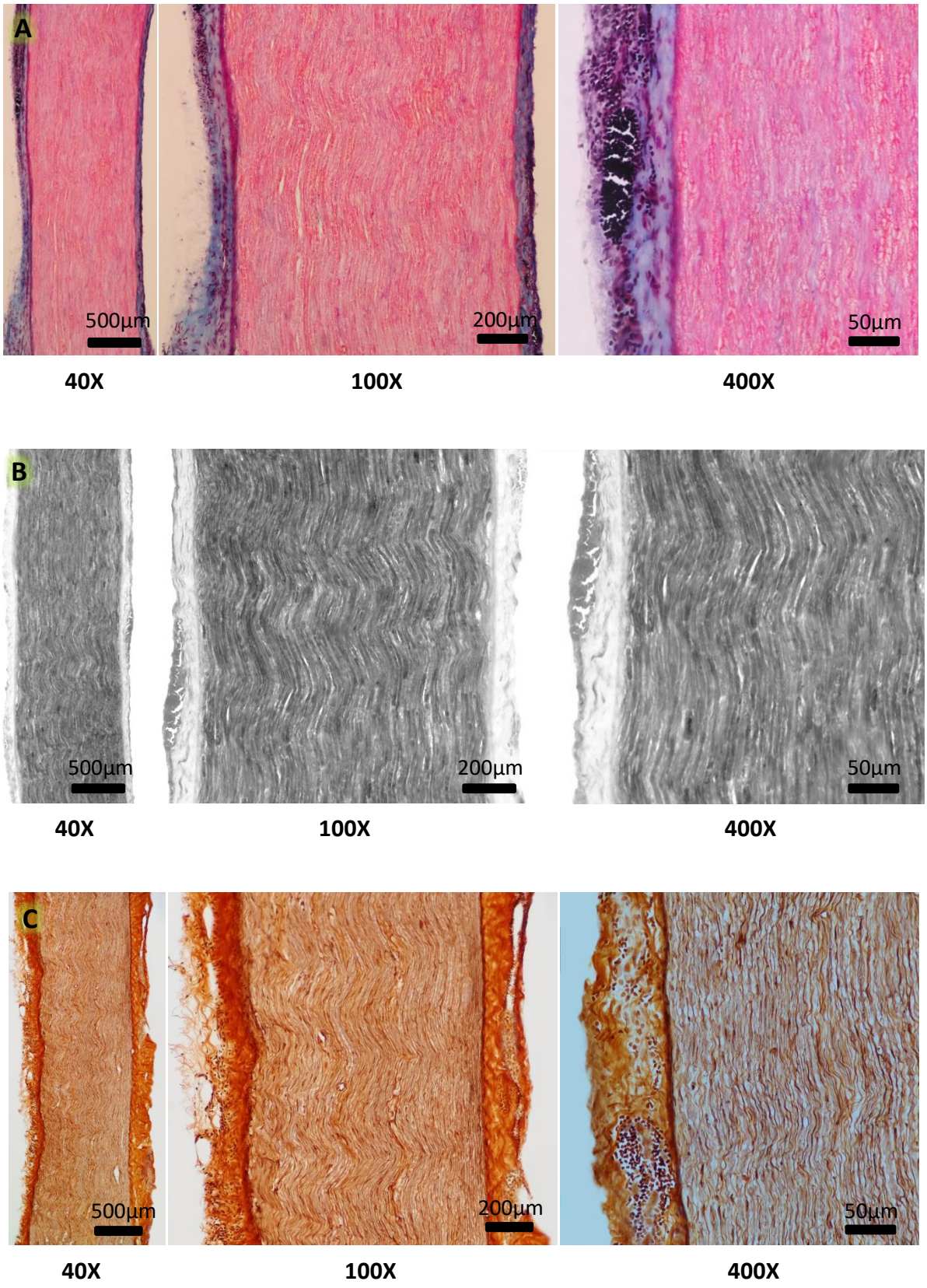

Figure 26: CelGro wrap 8 weeks post-surgery histology, longitudinal section

A. Masson's trichrome stain (preserved nerve histology, no apparent hypercellularity within nerve, membrane material largely disintegrated)
B. Osmium stain (preserved nerve histology, normal myelinated axon continuity, membrane material largely disintegrated)
C. Silver stain (preserved nerve histology, normal axon continuity, membrane material largely disintegrated)

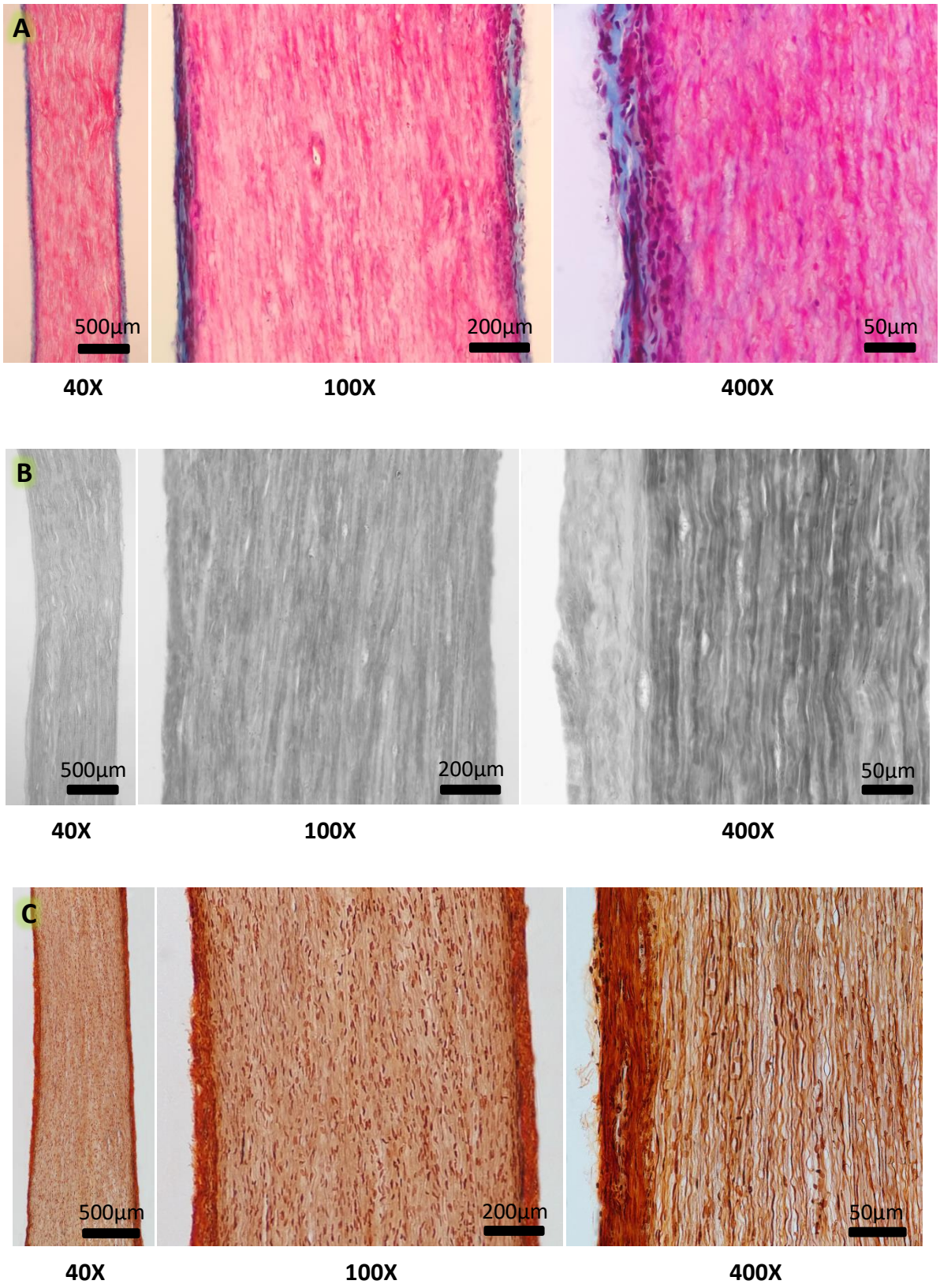

Figure 27: CelGro repair 8 weeks post-surgery histology, longitudinal section

A. Masson's trichrome stain (well recovered nerve histology, minimal hypercellularity, membrane material almost disintegrated)
B. Osmium stain (preserved nerve histology, myelinated axons largely regrown, membrane material almost disintegrated)
C. Silver stain (preserved nerve histology, axons largely regrown, membrane material almost disintegrated)

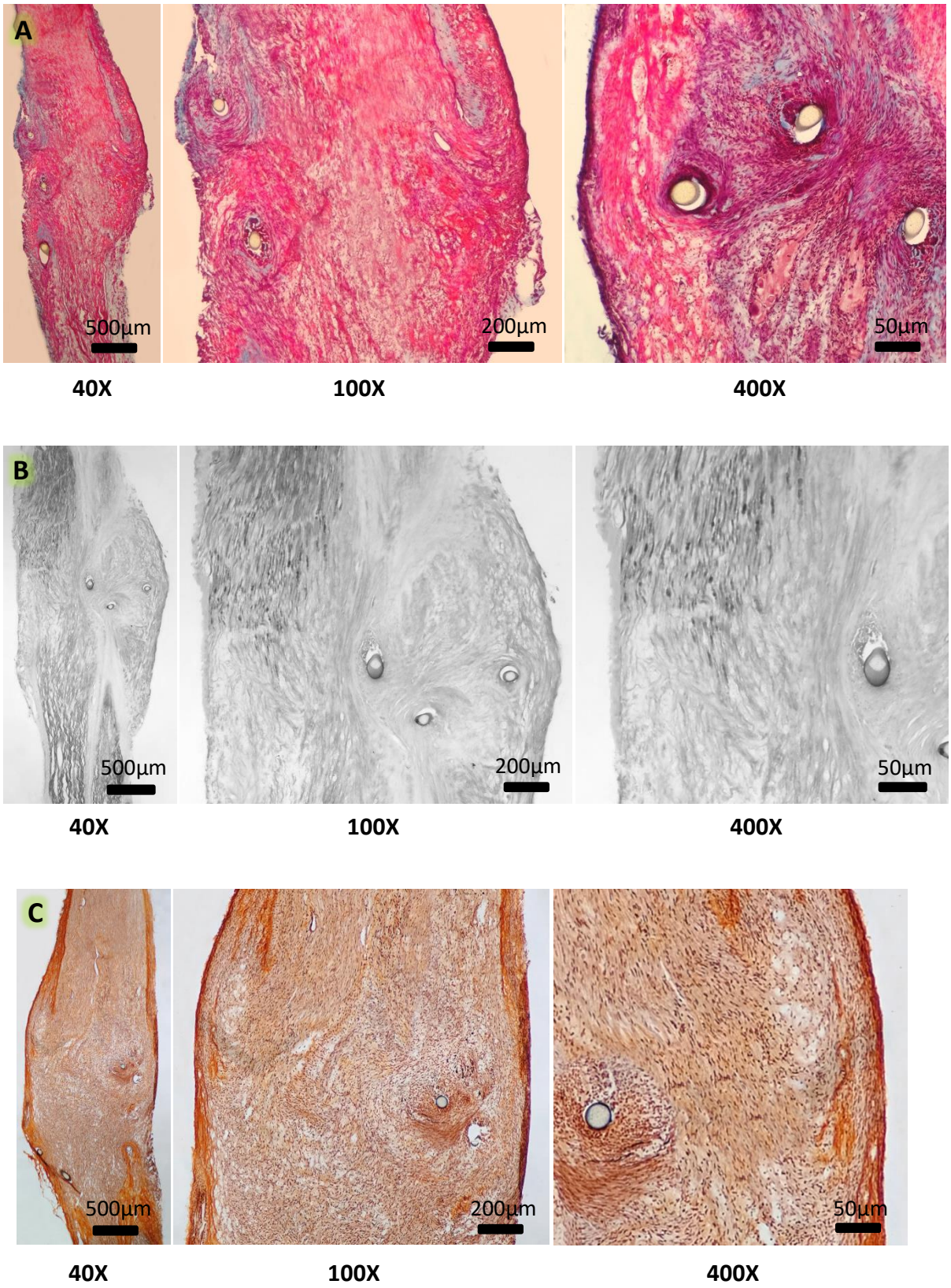

Figure 28: Suture repair 8 weeks post-surgery histology, longitudinal section

A. Masson's trichrome stain (heavily distorted nerve histology, axons growth disordered, substantial connective tissue deposition, appearance of neuroma-in-continuity)
B. Osmium stain (heavily distorted nerve histology, myelinated axons growth disordered, myelination incomplete around sutures, appearance of neuroma-in-continuity)
C. Silver stain (heavily distorted nerve histology, axons growth disordered especially around sutures, connective tissue deposition apparent, appearance of neuroma-in-continuity)

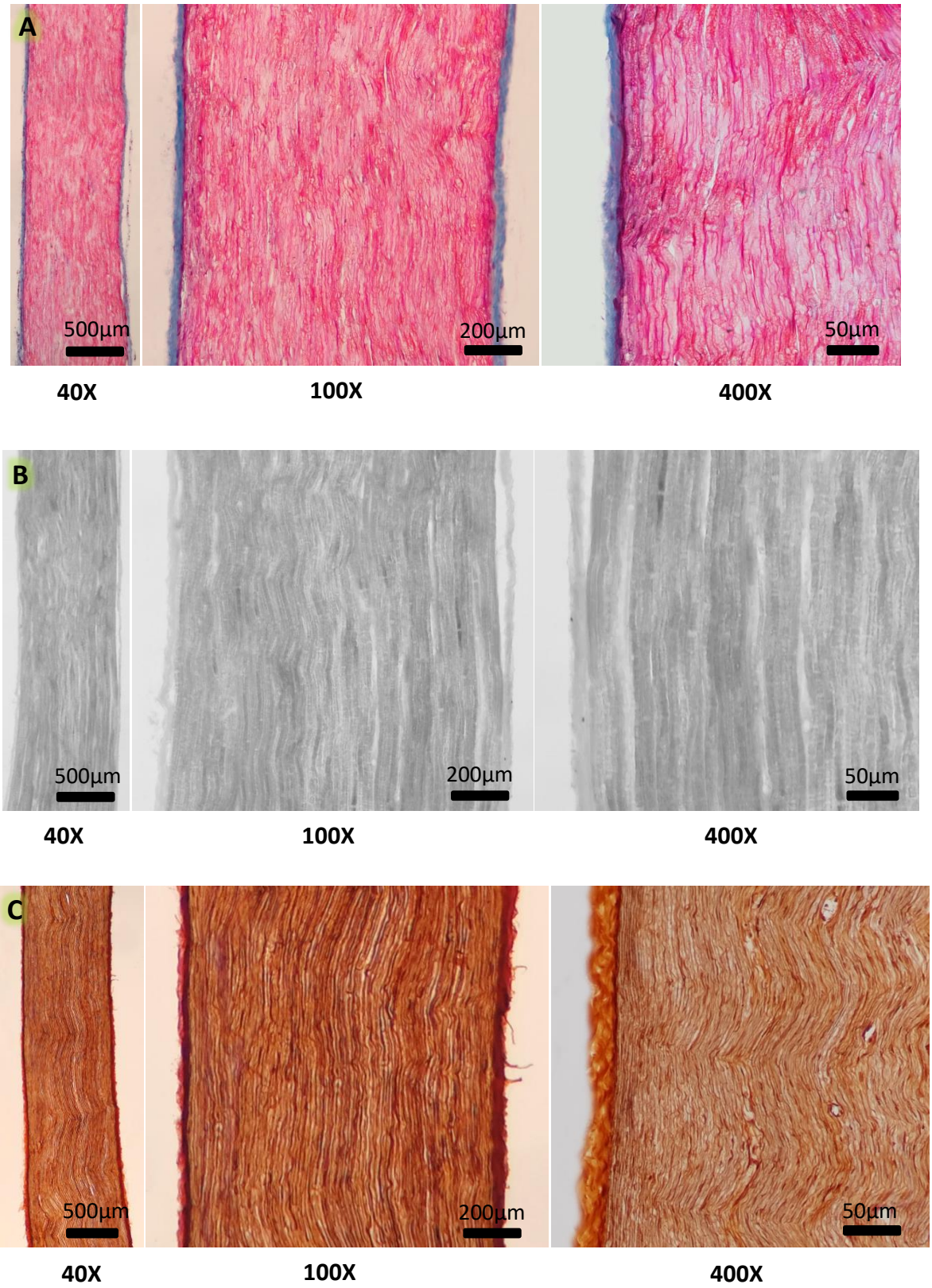

Figure 29: CelGro wrap 17 weeks post-surgery histology, longitudinal section

A. Masson's trichrome stain (normal nerve histology, no apparent hypercellularity within nerve, membrane material completely disintegrated)
B. Osmium stain (normal nerve histology, myelinated axons preserved, membrane material completely disintegrated)
C. Silver stain (normal nerve histology, axons structure preserved, membrane material completely disintegrated)

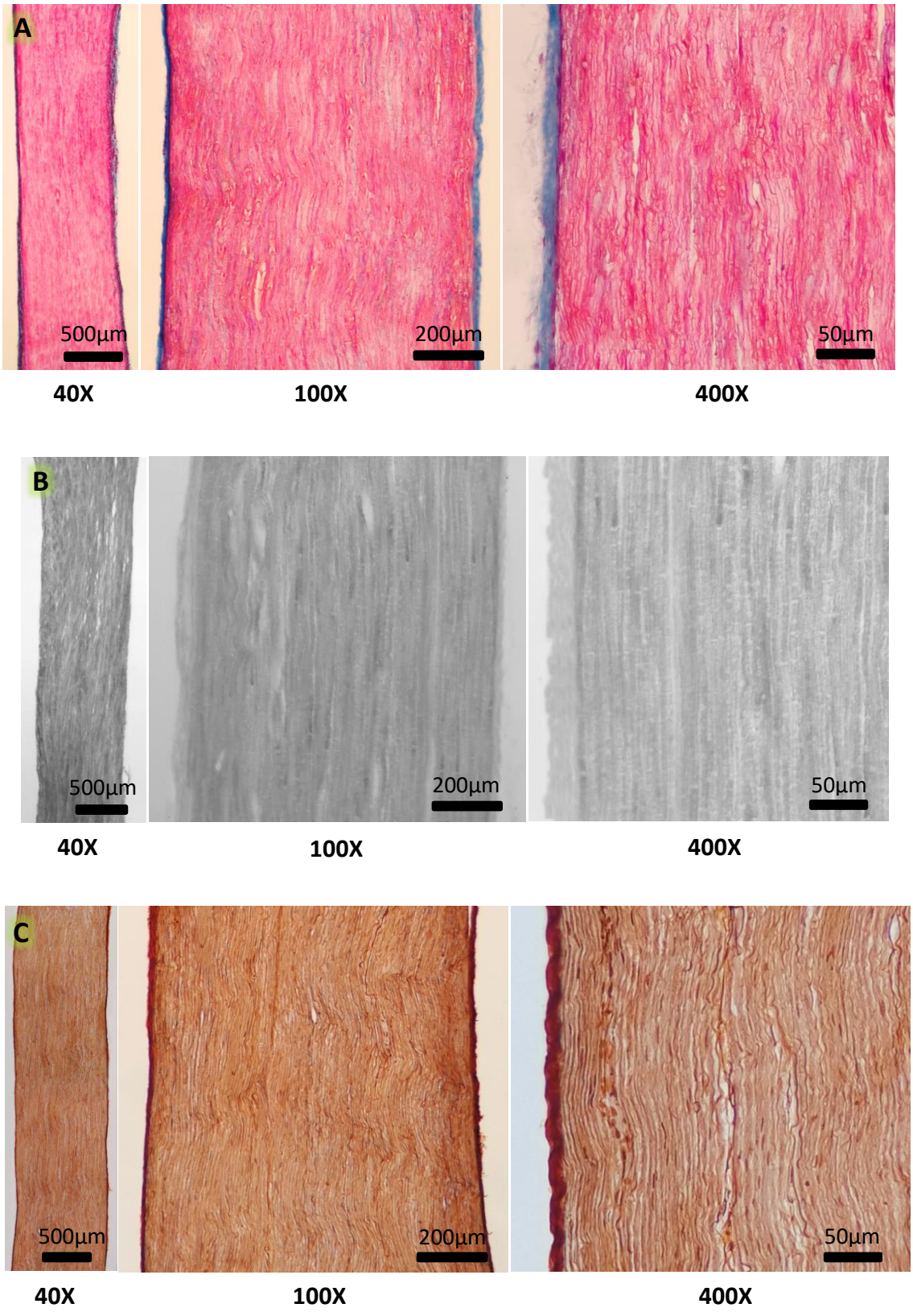

Figure 30: CelGro repair 17 weeks post-surgery histology, longitudinal section

A. Masson's trichrome stain (virtually normal nerve histology, membrane material completely disintegrated)
B. Osmium stain (virtually normal nerve histology, myelinated axons almost completely regrown)
C. Silver stain (virtually normal nerve histology, axons threads almost completely regrown)

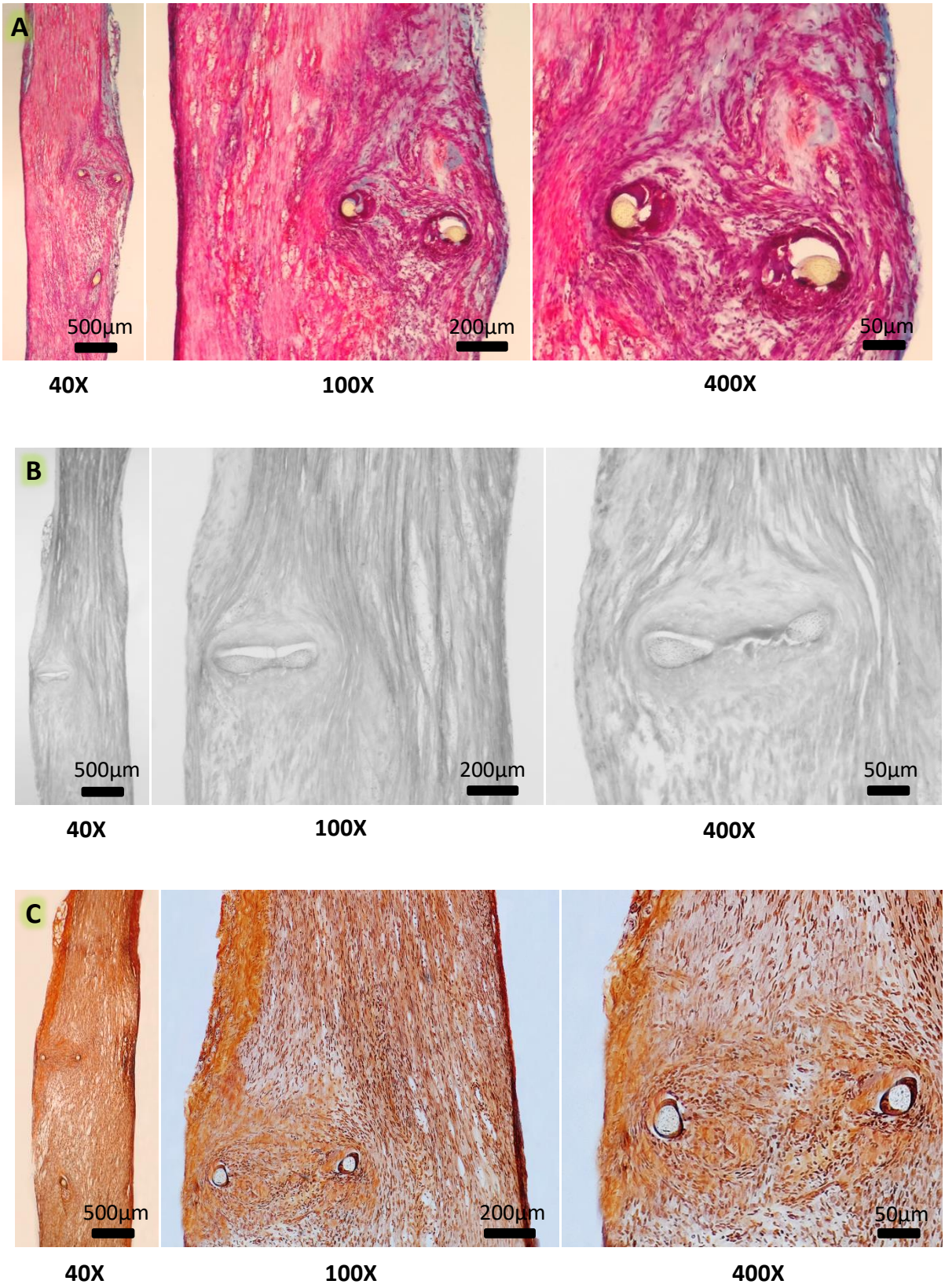

Figure 31: Suture repair 17 weeks post-surgery histology, longitudinal section

A. Masson's trichrome stain (nerve histology only partially recovered, substantial connective tissue deposition in nerve, aberrant axon growth, appearance of neuroma-in-continuity)
B. Osmium stain (nerve histology only partially recovered, disordered regrowth of myelinated axons, poor myelination around sutures, appearance of neuroma-in-continuity)
C. Silver stain (nerve histology only partially recovered, incomplete and irregular regrowth of axon threads, substantial connective tissue deposition, appearance of neuroma-in-continuity)

5. Discussion

Suturing is still the standard surgical treatment technique for nerve transection injuries and has not fundamentally changed for decades (Panagopoulos, Megaloikonomos & Mavrogenis 2017). Non-absorbable monofilament nylon suture is traditionally chosen by most surgeons because of reduced foreign-body reactivity associated with its placement (Lee & Wolfe 2000), even though others have found no functional and histological differences between absorbable and non-absorbable sutures (Cham et al. 1984, Murray, Willins & Mountain 1994). Regardless, nerve suturing (neurorrhaphy) requires considerable skills and experience, is time consuming, and has several disadvantages such as manipulation-induced further nerve trauma, foreign body inflammatory reaction with scarring, and tension/compression at a coaptation site that interferes with axonal growth/alignment (Griffin et al. 2013). Intraneural scarring is of a particular concern, and over the years various surgical and pharmacological measures have been tried to reduce it, with variable and, generally, unsatisfactory results (Ngeow 2010, Saied et al. 2015). Several sutureless techniques are increasingly being examined as potentially superior in regard to complexity and clinical outcomes (Barton et al. 2014). Rose-Bengal dye and laser light have been investigated in repair of injuries affecting cornea (Mulroy et al. 2000), skin (Xu et al. 2015), tendon (Chan et al. 2005), blood vessels (O'Neill et al. 2007) and vocal folds (Franco et al. 2011). This photobonding method has also been applied in nerve repair, in conjunction with chitosan membranes (Barton et al. 2015) and human amniotic membranes (O'Neill et al. 2009) as scaffolding materials.

ECM produced from several types of animal tissue is becoming increasingly popular biological scaffold in regenerative medicine (Parmaksiz et al. 2016). One of those materials is CelGro, derived from porcine peritoneum and marketed by Orthocell. So far CelGro collagen membranes have been used in in a combination with sutures, but this study has managed to demonstrate that CelGro can be successfully bonded to intestine and nerve tissue with laser-activated Rose-Bengal solution as adhesive, using a protocol already described for fabricated chitosan-RB films (Lauto et al. 2010). In this method Rose-Bengal reacts with laser light of 532 nm wavelength producing cross-linking of proteins through a still incompletely understood mechanism. It is likely mediated via electron transfer between the reactive species produced during the photoactivation process, such as singlet oxygen molecules, free radicals, and

peroxides, with collagen amino acid residues such as arginine, tryptophan, histidine and tyrosine (Alarcon et al. 2017, Au & Madison 2000, Chan et al. 2007, Webster et al. 1989).

CelGro membranes displayed greater bonding strength when their smooth side was positioned against the tissue surface, possibly because the smooth texture offers a flatter surface area for bonding than the rough side, as evidenced on light microscopy. CelGro membranes appear to have comparable adhesion strength to the chitosan-RB films, when tested in vitro on cut intestinal tissue sections, under the identical photobonding conditions. This was in spite of CelGro membrane being considerably thicker (around 3-4 times) and less transparent than the chitosan-RB film, which would reduce laser light penetration to the membrane/tissue interface. Additionally, there is a reason to believe that laser-welded CelGro+RB would be superior to laser-welded chitosan-RB in tensile testing on repaired nerves due to the double wrapped CelGro membrane shrinking around the nerve ends during laser irradiation and thus exerting additional mechanical grip. While this remains to be quantified, this study showed consistently strong and effective connection of the nerve stumps with the CelGro membrane, with no bond failure. To the best of my knowledge this shrinking process has not been described in literature so far. It seems to occur as a result of shape change and shortening of collagen fibres/bundles in a mesh-like membrane structure, presumably developing by the same RB-mediated mechanism that underlies membrane-tissue bonding. This is supported by the observation that no shrinking occurs when the membrane is painted with saline only (without RB) and then exposed to laser light.

Currently, in complete peripheral nerve injuries where nerve stumps can be brought together without excessive tension, primary (surgical term for immediately after injury) end-to-end repair with sutures is believed to offer the best clinical prognosis (Griffin et al. 2014). Outcome of such surgery, which depends considerably on the surgeon's skills, can be hindered by imperfect fascicular alignment of the nerve stumps, consequently resulting in perineural and intraneural fibrosis. This study has explored an alternative sutureless method for primary end-to-end repair that is arguably easier to learn and perform, and, very importantly, avoids additional traumatic nerve injury associated with nerve handling and suture placement. On top of that, no artificial material is retained within the nerve tissue in the long run, eliminating foreign body inflammatory reaction and resultant scarring that may follow. These processes

can result in impediment to the regenerating axons that need to successfully traverse the injury site, thus reducing functional recovery (Eather, Pollock & Myers 1986, Ngeow 2010).

In this study, the operator who placed and bonded the CelGro membranes around the transected nerves did not possess specialised training in microneurosurgery or plastic surgery. Despite that the technique was found to be relatively easy to master with minimal training. Very little nerve handling was needed, and no needles were required to be threaded through nerve structures. Alignment of the nerve stumps proved much easier to achieve during the CelGro placement compared to suturing. This is important since it has been accepted that misalignment of the motor and sensory axons during nerve repair is one of the biggest barriers for good functional recovery, as many axons do not reach their distal targets, or reach the wrong destinations (Madison et al. 1999). No bond failure and nerve stump separation was experienced, despite the experimental animals returning to mobility very shortly after surgery. In human surgical practice repaired nerves are typically protected by immobilisation for around two weeks or more depending on the severity of nerve injury and its cause (Mackinnon & Dellon 1988). Such resting conditions would further improve the outcomes of tissue and nerve repair.

Wrapping a CelGro membrane around intact nerves (sham) produced a transient paw hypersensitivity to mechanical and thermal stimuli lasting approximately 3 weeks, likely as a consequence of peripheral or central sensitisation resulting from nerve exposure, manipulation and exposure to laser irradiation (Shaikh et al. 2016). It is possible that a shrinking membrane cuff also produced minor transient nerve compression. Sciatic nerve transection induced immediate anaesthesia lasting 4 weeks, after which the rats started to respond to mechanical and thermal nociceptive stimuli due to nerve regeneration, and subsequently developed hyperaesthesia that slowly retuned to baseline values. These findings are mostly consistent with those already published in literature (Cobianchi et al. 2014, Casals-Díaz, Vivó & Navarro 2009, Wood et al. 2011). This 4-week period coincides with the time needed for regenerating axons to reach their peripheral targets, growing at a reported rate or around 1-2 mm/day (Grinsell & Keating 2014, Menorca, Fussell & Elfar 2013). Sciatic re-innervation was followed by mechanical and thermal hyperaesthesia that reverted slowly over time (Vogelaar et al. 2004, Cobianchi, de Cruz & Navarro 2014). The most likely explanation for this apparent hypersensitivity (hyperalgesia and allodynia) is reduced

threshold of regenerated sensory nerve fibres to mechanical and thermal stimuli (Jankowski et al. 2009). Peripheral sprouting from the saphenous nerve from the medial edge of the paw is an unlikely mechanism of this hypersensitivity due to such delayed onset and the fact that sensory testing was performed along the lateral side of the plantar paw surface where no saphenous sprouting would reach (Cobianchi, de Cruz & Navarro 2014).

When compared to suturing, the photochemically bonded collagen membrane method displayed faster sensory recovery throughout the entire observation period of 17 weeks. CelGro repaired nerves demonstrated faster recovery from initial anaesthesia and reached less marked hyperesthesia. Return to normal sensation from this hyperaesthesia was identified 2-3 weeks earlier with CelGro repair compared to suture repair, which would certainly have a value in a clinical setting. This is consistent with better regeneration of sensory axons and/or their more effective reconnection with the peripheral targets, as well as more effective resolution of nerve fibre hypersensitivity. However, at the very end of the experiment period (17 weeks) there was no significant difference in response to sensory stimuli between the two repair methods, as both eventually reached their respective baseline levels. This was at odds with sub-optimal histological appearance of the sutured nerves which invariably showed histologically intraneural scarring with some fascicular misalignment and disordered axonal growth. It should be mentioned that the used sensory tests only measured withdrawal responses to mechanical and thermal stimuli, so it is unknown whether there was any difference in recovery of the other sensory modalities, such as fine touch, two-point discrimination and stereognosis, which are routinely tested in clinical practice (Wang, Sunitha & Chung 2013). This testing would be very difficult to conduct accurately and reliably on laboratory animals and only human clinical trials would shed light on this clinically important question. Sensory testing on humans would generally follow standard neurologic assessment procedure and typically include testing for vibration with tuning forks, fine touch with von Semmes Weinstein filaments and two-point discrimination with the discriminator tools.

In regards to motor function, at the end of the experiment, animals with CelGro repaired nerves had 32% higher gastrocnemius compound muscle action potential and 22% greater gastrocnemius weight than the suture group. According to Navarro (2016) the amplitude of the CMAP is determined by the number of muscle fibres innervated, and it is the most useful indicator for nerve regeneration studies. Similarly, weight of the gastrocnemius muscle is

thought to be proportional to the level of innervation, considering that denervated muscles develop atrophy due to decrease of muscle fibre diameter, which progresses in time. Wet weight of rat gastrocnemius muscles was reported to be 25–32% of that of the contralateral side 4 months after complete denervation without repair (Schmalbruch et al., Wu et al. 2014). This study has found that 4 months post-surgery CelGro repaired nerves preserved 63% of the contralateral control muscle weight, while suture repaired nerves showed 52% of the contralateral control muscle weight. These results suggest better motor axon re-innervation after CelGro repair, and are promising from a clinical perspective, especially if this advantage can be sustained over a longer period of time as muscle function continues to improve. Nonetheless, this study did not incorporate behavioural muscle strength testing in vivo (such as extensor postural thrust test), which would be valuable in assessing temporal functional motor recovery throughout the 17-week observation period.

As the axons grow distally from the point of transection and reach the appropriate target tissues, axons diameter progressively increases and the myelin sheath progressively thickens (Myles & Glasby 1991, Muratori et al. 2012). At the end of the experiment (17 weeks), compared to intact nerves CelGro repaired nerves had similar thickness in the repaired area, which suggests favourable axonal regeneration and myelination. In contrast, sutured nerves were 12% thicker around the transection line than the intact nerves. One explanation for this observation is presence of intraneural/epineural scarring in suture repaired axons (as observed on histology). It has been demonstrated that after sciatic nerve transection there is an initial increase in the number of axons distal to the site of transection, followed by a gradual decrease through degeneration of those that do not manage to make an appropriate connection with the target organ (Mackinnon et al. 1991). Suture repaired nerves could have had greater number of axon sprouts, possibly due to improper fascicular alignment and connective tissue barriers, many of which will slowly degenerate over the following several months after they do not achieve effective linking with the peripheral organs (Ikeda & Oka 2012). However, in this study no axon count was performed to assess this possibility.

CelGro membrane wrapping seems to be well tolerated by intact nerves, as no intraneural inflammatory response was observed, as evidenced by lack of hypercellularity in the subepineurium regions. Most of the material was dissolved by week 8 post-surgery, with no residual material evident at week 17. No perineural scarring and adhesions with the

surrounding muscles were found during nerve harvesting. Similar membrane biodegradability and absence of adhesions were observed with CelGro repaired nerves as well. Restoration of microscopical histological structure of CelGro repaired nerves was markedly superior to the sutured nerves. There was distinctly better nerve stump/fascicular alignment, less intraneural hypercellularity, more effective straight axonal growth and virtually no intraneural scarring. At the end of this 17-week period there was almost no structural histological difference between the normal nerves, CelGro wrapped normal nerves and CelGro repaired transected nerves. Such good healing of CelGro repaired nerves was very encouraging and provides a solid basis for good functional recovery.

In contrast, all sutured nerves showed some degree of axon growth disorganisation/ misdirection and intraneural fibrosis, especially around the placed sutures. Fascicular misalignment and presence of fibrosis is of a particular concern as it can be a substantial barrier to effective axon regrowth, forcing excessive non-functional sprouting and neuroma formation (Atkins et al. 2006, Lundborg 1987). A neuroma is a fibroneural mass containing disorganised axons, connective tissue, together with the cells such as Schwann's cells, macrophages and fibroblasts. Neuroma-in-continuity forms inside the nerve as a result of failure of the regenerating axon sprouts to reach peripheral targets (Kline 1982, Mavrogenis et al. 2008). Histologic changes consistent with neuroma-in-continuity have been observed in all sutured nerves. Such neuromas would interfere with functional recovery and could produce long-term neurologic deficit and neuropathic pain. Additional problem is the presence of perineural scarring and formation of adhesions observed with the sutured nerves. It has been demonstrated that such adhesions between the nerve and its surrounding tissue substantially limit the gliding/elongation of the nerve during normal body movements, which can cause intraneural ischaemia and chronic neuropathy, sometimes referred to as ‘scar neuritis’ (Elliot 2014, Tos et al. 2015).

Due to their small size, rat sciatic nerves (comparable in size to human digital nerves) proved challenging in regard to surgical repair and placement of epineurial sutures, even with the help of an operating microscope in hands of experienced plastic surgeon. Some of the sutures were accidentally positioned deeper into the nerve where they interfered with axon budding, as evidenced histologically by axons being forced to grow around the sutures. It could be argued that the histological results could have been better if larger nerves were repaired and

a more skilled/careful neurosurgical technique was employed to ensure the optimal suture position. Microneurosurgical technique has a steep learning curve and requires considerable experience and time to produce good clinical outcomes (Whitlock et al. 2010). It could be argued that surgeries performed in this experiment are probably quite representative of the surgical practice at work in majority busy operating theatres, where time is at a premium and where availability of microneurosurgical expertise can vary.

Overall, photochemically bonded collagen membrane proved to be a viable alternative to standard surgical suture-based primary end-to-end repair. It does not require microsurgical suturing skills and would work well even if the nerve stumps cannot be fully approximated without substantial tension, which is often unavoidable as the nerve stumps typically retract somewhat even after a clean cut. This novel method produces demonstrably better macroscopic and microscopic healing of transected nerves, and faster/better functional recovery in regard to sensory and motor function. Additionally, this method could be faster to perform than suturing and consequently may be able to save valuable time in operating theatres. More research is needed to find out if this is indeed the case. This is relevant as a recent survey of surgeon perspectives on alternative nerve repair techniques has found that over 90% of the surveyed surgeons reported that they either currently use or would consider using sutureless techniques, especially if they are faster and easier in practice (Owusu, Mayeda & Isaac 2014).

It should be noted that the employment of a Class 4 laser device (used in this research) imposes certain health hazards and is subject to strict safety guidelines which include mandatory operator training, wearing prescribed eye protection and restricted access to the room while laser use is in progress. This could be seen as a potential barrier for adoption in clinical practice. One way to address this limitation would be to explore the use of LED light of similar wavelength and power characteristics, which does not have the same health concerns and would require less expensive apparatus.

In conclusion, the results presented in this thesis have demonstrated that:

1. CelGro collagen membranes can be successfully photochemically bonded to tissue with Rose-Bengal solution as adhesive and 532 nm green laser for its activation. Photochemically bonded CelGro membranes achieve comparable bonding strength

to photochemically bonded chitosan-RB films that have already been successfully used in sutureless nerve repair.

2. Photochemically bonded CelGro membranes do not seem to induce visible foreign body style inflammatory reaction, and progressively become degraded over the period of around 2 months.
3. CelGro repaired nerves show better sensory and motor functional recovery than suture repaired nerves, which could translate into better clinical outcomes.
4. CelGro repaired nerves demonstrate superior histology over suture repaired nerves, in relation to fascicular alignment, axon regeneration and development of intraneural and perineural scarring. Importantly no neuroma-in-continuity changes have been observed with CelGro repaired nerves, unlike the suture repaired ones, reducing the likelihood of chronic neuropathic pain.

6. Future work

This study has evaluated recovery of sensory functions, but did not look into behavioural assessment of motor activity of the hind limbs. Consequently, employing suitable methods for assessing motor functions, such as SFI and EPT tests, would shed additional light on dynamics and outcomes of the nerve repair assisted by CelGro membranes. Further valuable information could be obtained with more detailed electrophysiological testing, including CMAP latencies and nerve conduction velocities.

Histological methods used in this study were largely qualitative and focused on axonal regeneration, as well as connective tissue proliferation in regard to extraneural and intraneural scarring. More objective assessment of axonal regeneration would be possible with axonal counting on transverse nerve sections below the transection line, such as methylene blue stained semithin sections after resin embedding. Quantification of fibrosis could be obtained through computerised digital image analysis by measuring the intensity of blue colour which represents the collagen density in Masson's trichrome staining. Also, routine histological staining procedures utilised here did not allow precise identification of the cells observed on light microscopy, and only assumptions could be made about their type. Immunohistology techniques could be employed to show the presence and proliferation of Schwann cells, macrophages and fibroblasts, which would be of value in assessing the inflammatory and regeneration processes after nerve repair (Kaemmer et al. 2010, Pilling et al. 2009). A particular point of interest is whether inflammation process in CelGro repaired nerves is less intense and of shorter duration than in suture repaired nerves.

Next research step is an application of photochemically bonded collagen membranes in repair of gap injuries of peripheral nerves, as opposed to surgical practice of autologous nerve grafting (obtained from the patient) and commercially available fabricated nerve guidance conduits (NGCs). Such nerve injuries are most commonly encountered in clinical practice and present substantial challenges in relation to treatment and recovery. For example, sural nerve autografts, which is the gold standard for nerve defects longer than 5mm, have demonstrated very modest functional recovery rates, especially in treatment of motor or mixed nerve injuries (sural nerve is mainly sensory) (Daly et al. 2012). Currently NGCs used in clinical practice are primarily made from synthetic materials such as poly-glycolic acid and

polylactide-caprolactone, or from cross-linked animal collagen I (Daly et al 2012). While they avoid donor-site morbidity associated with harvesting nerve grafts (neuroma formation, loss of function), none of them was shown to produce better functional recovery than autografting (Pabari et al. 2014).

It is envisaged that using CelGro to repair nerve defects will have to include development of a suitable process for making a membrane conduit 'in situ' around the injured nerve, that would result in a strong, flexible and patent tube. Such process could be an improvement over prefabricated conduits that typically come in a limited selection of fixed diameters. More research is needed to show how competitive this technique would be with the established surgical practices in human medicine in regard to required level of skill, clinical outcomes and cost-effectiveness.

References

Abrams, RA, Butler, JM, Bodine-Fowler, S & Botte, MJ 1998, 'Tensile properties of the neurorrhaphy site in the rat sciatic nerve', The Journal of Hand Surgery, vol. 23, no. 3, pp. 465-470.

Alant, JD, Kemp, SW, Khu, KJ, Kumar, R, Webb, AA & Midha, R 2012, 'Traumatic neuroma in continuity injury model in rodents', Journal of Neurotrauma, vol. 29, no. 8, pp. 1691-1703.

Alarcon, EI, Poblete, H, Roh, H, Couture, J, Comer, J & Kochevar, I 2017, 'Rose Bengal Binding to Collagen and Tissue Photobonding', ACS Omega, vol. 2, pp. 6646-6657.

Atkins, S, Smith, KG, Loescher, AR, Boissonade, FM, O'Kane, S & Ferguson, MW 2006, 'Scarring impedes regeneration at sites of peripheral nerve repair', Neuroreport, vol. 17 pp: 1245-1249.

Au, V & Madison, SA 2000, 'Effects of singlet oxygen on the extracellular matrix protein collagen: oxidation of the collagen crosslink histidinohydroxylysinonorleucine and histidine', Archives Biochemistry Biophysics, vol. 384, pp. 133–142.

Badylak, SF, Freytes, DO & Gilbert, TW 2009, 'Extracellular matrix as a biological scaffold material: Structure and function', Acta Biomaterialia, vol. 5, no. 1, pp. 1–13.

Bamba, R, Riley, DC, Kelm, ND, Cardwell, N, Pollins, AC, Afshari, A, Nguyen, L , Dortch, RD, Thayer, WP 2017, 'A novel conduit-based coaptation device for primary nerve repair', International Journal of Neuroscience, vol. 128, no. 6, pp. 563–569.

Bain, JR, Mackinnon, SE & Hunter, DA 1989, 'Functional evaluation of complete sciatic, peroneal and posterior tibial nerve lesions in the rat', Plastic and reconstructive surgery, vol. 83, no. 1, pp. 129-138.

Bancroft, JD & Layton, C 2013 'Connective and mesenchymal tissues with their stains' in Suvarna, KS, Layton, S. & Bancroft, JD (eds), *'Bancroft's Theory and Practice of Histological Techniques'*, Edinburgh, Churchill Livingstone Elsevier, pp. 199-205.

Barton, M, Morley, JW, Stoodley, MA, Shaikh, S, Mahns, DA & Lauto, A 2015, 'Long term recovery of median nerve repair using laser-activated chitosan adhesive films', Journal of Biophotonics, vol. 8, no. 3, pp. 196-207.

Barton, M, Morley, JW, Stoodley, MA, Ng, KS, Piller, SC, Duong, H, Mawad, D, Mahns, DA & Lauto A 2013, 'Laser-activated adhesive films for sutureless median nerve anastomosis', Journal of Biophotonics, vol. 6, no. 11-12, pp. 938-949.

Barton, M, Morley, JW, Stoodley, MA, Lauto, A & Mahns, DA 2014, 'Nerve repair: toward a sutureless approach', Neurosurgical Review, vol. 37, no. 4, pp. 585-595.

Benders, KE, van Weeren, PR, Badylak, SF, Saris, DB, Dhert, WJ & Malda, J 2013, 'Extracellular matrix scaffolds for cartilage and bone regeneration', Trends in Biotechnology, vol. 31, no. 3, pp. 169-176.

Bourne, S, Machado, AG & Nagel, SJ 2014, 'Basic anatomy and physiology of pain pathways', Neurosurgery Clinics of North America, vol. 25, no. 4, pp. 629-638.

Brushart, TM, Gerber, J, Kessens, P, Chen, YG & Royall, RM 1998, 'Contributions of pathway and neuron to preferential motor reinnervation', Journal of Neuroscience, vol. 18, pp. 8674–8681.

Caillaud, M, Richard, L, Vallat, JM, Desmoulière, A & Billet, F 2019, 'Peripheral nerve regeneration and intraneural revascularization', Neural Regeneration Research, vol. 14, no. 1, pp. 24-33.

Campbell, WW 2008, 'Evaluation and management of peripheral nerve injury', Clinical Neuro Physiology, vol. 119, no. 9, pp. 1951-1965.

Casals-Díaz, L, Vivó, M & Navarro, X 2009, 'Nociceptive responses and spinal plastic changes of afferent C-fibers in three neuropathic pain models induced by sciatic nerve injury in the rat', Experimental Neurology, vol. 217, no. 1, pp. 84–95.

Cham, R, Peimer, CA, Howard, CS & Eckert, B 1984, 'Absorbable versus nonabsorbable suture for microneurorrhaphy', The Journal Of Hand Surgery, vol. 9, no. 3, pp. 434-440.

Chan, BP, Kochevar, IE & Redmond, RW 2002, 'Enhancement of Porcine Skin Graft Adherence Using a Light-Activated Process', Journal of Surgical Research, vol. 108, pp. 77–84.

Chan, BP, Amann, C, Yaroslavsky, AN, Title, C, Smink, D, Zarins, B, Kochevar, IE & Redmond, RW 2005, 'Photochemical repair of Achilles tendon rupture in a rat model', Journal of Surgical Research, vol 124, no. 2, pp: 274-279.

Chan, BP, Hui, TY, Chan, OC, So, KF, Lu, W, Cheung, KM, Salomatina, E &Yaroslavsky, A. 2007, 'Photochemical cross-linking for collagen-based scaffolds: a study on optical properties, mechanical properties, stability, and hematocompatibility', Tissue Engeneering, vol. 13, no. 1, pp. 73-85.

Chen, P, Piao, X & Bonaldo, P 2015, 'Role of macrophages in Wallerian degeneration and axonal regeneration after peripheral nerve injury', Acta Neuropathologica, vol. 130, no. 5, pp. 605-618.

Cherfan, D, Verter, EE, Melki, S, Gisel, TE, Doyle, FJ, Scarcelli, G et al. 2013, 'Collagen cross-linking using rose bengal and green light to increase corneal stiffness', Investigative ophthalmology & visual science, vol. 54, no. 5, pp. 3426-3433.

Ciardelli, G & Chiono, V 2006, 'Materials for Peripheral Nerve Regeneration', Macromolecular Bioscience, vol. 6, no. 1, pp. 13-26.

Clark, WL, Trumble, TE, Swiontkowski, MF & Tencer, AF 1992, 'Nerve tension and blood flow in a rat model of immediate and delayed repairs', The Journal of Hand Surgery, vol. 17, no. 4, pp. 677–687.

Cobianchi, S, de Cruz, J & Navarro, X 2014, 'Assessment of sensory thresholds and nociceptive fiber growth after sciatic nerve injury reveals the differential contribution of collateral reinnervation and nerve regeneration to neuropathic pain', Experimental Neurology, vol. 255, pp. 1–11.

Cruz, NI, Debs, N & Fiol, RE 1986, 'Evaluation of fibrin glue in rat sciatic nerve repairs', Plastic and reconstructive surgery, vol. 78, no. 3, pp. 369-373.

Dahlin, IB 2008, 'Techniques of peripheral nerve repair', Scandinavian Journal of Surgery, vol. 97, no. 4, pp. 310–316.

Daly, W, Yao, L, Zeugolis, D, Windebank, A & Pandit, A 2012, 'A biomaterials approach to peripheral nerve regeneration: bridging the peripheral nerve gap and enhancing functional recovery', Journal of the Royal Society of London Interface, vol. 9, no. 67, pp. 202-221.

Danielsen, N & Varon, S 1995, 'Characterization of neurotrophic activity in the silicone-chamber model for nerve regeneration', Journal of Reconstructive Microsurgery, vol. 11, no. 3, pp. 231–235.

De Koning, P, Brakkee, JH & Gispen, WH 1986, 'Methods for producing a reproducible crush in the sciatic and tibial nerve of the rat and rapid and precise testing of return of sensory function: Beneficial effects of melanocortins', Journal of the Neurological Sciences, vol. 74, no. 2–3, pp. 237-246.

De Luca, A, Raffoul, W, Giacalone, F, Bertolini, M & Di Summa, P 2015, 'Tissue‐engineered constructs for peripheral nerve repair: current research concepts and future perspectives', Plastic and Aesthetic Research, vol. 2, no. 4, pp. 213-217.

De Medinaceli, L , Freed, WJ & Wyatt, RJ 1982, 'An index of the functional condition of rat sciatic nerve based on measurements made from walking tracks', Experimental Neurology, vol. 77, pp. 634-643.

Deumens, R, Bozkurt, A, Meek, MF, Marcus, M, Joosten, E, Weis, J & Brook, GA 2010, 'Repairing injured peripheral nerves: Bridging the gap', Progress in Neurobiology, vol. 92, pp. 245–276.

Diao, E, Vannuyen, T 2000, 'Techniques for primary nerve repair', Hand Clinics, vol. 16, no. 1, pp. 53-66.

Djouhri, L & Lawson, SN 2004, 'Aβ-fiber nociceptive primary afferent neurons: A review of incidence and properties in relation to other afferent A-fiber neurons in mammals', Brain Research Reviews, vol. 46, no. 2, pp 131-145.

Dubin, AE & Patapoutian, A 2010, 'Nociceptors: the sensors of the pain pathway', Journal of Clinical Investigation, vol. 120, no. 11, pp. 3760–3772.

Ducic, I, Fu, R & Iorio, ML 2012, 'Innovative treatment of peripheral nerve injuries: combined reconstructive concepts', Annals of Plastic Surgery, vol. 68, no. 2, pp. 180–187.

Eather, TF, Pollock, M & Myers, DB 1986, 'Proximal and distal changes in collagen content of peripheral nerve that follow transection and crush lesions', Experimental Neurology, vol. 92, pp. 299-310.

Elliot, D 2014, 'Surgical management of painful peripheral nerves', Clinics in Plastic Surgery, vol. 41, pp. 589-613.

Evans, PJ, Mackinnon, SE, Best, TJ, Wade, JA, Awerbuck, DC, Makino, AP, Hunter, DA & Midha, R 1995, 'Regeneration across preserved peripheral nerve grafts', Muscle Nerve, vol. 18, pp. 1128–1138.

Fairbairn, NG, Ng-Glazier, J, Meppelink, AM, Randolph, MA, Winograd, JM & Redmond, RW 2016, 'Improving Outcomes in Immediate and Delayed Nerve Grafting of Peripheral Nerve Gaps Using Light-Activated Sealing of Neurorrhaphy Sites with Human Amnion Wraps', Plastic and reconstructive surgery, vol. 137, no. 3, pp. 887-895.

Félix, SP, Pereira Lopes, FR, Marques, SA & Martinez, AM 2013, 'Comparison between suture and fibrin glue on repair by direct coaptation or tubulization of injured mouse sciatic nerve', Microsurgery, vol. 33, no. 6, pp. 468-477.

Finnerup, N 2011, 'Mechanisms of dynamic mechanical allodynia and dysesthesia in patients with peripheral and central neuropathic pain', European Journal of Pain, vol. 15, no. 5, pp. 498-503.

Franco, RA, Dowdall, JR, Bujold, K, Amann, C, Faquin, W, Redmond, RW & Kochevar, IE 2011, 'Photochemical repair of vocal fold microflap defects', Laryngoscope, vol. 121, no. 6, pp.1244-1251.

Gaudet, AD, Popovich, PG & Ramer, MS 2011, 'Wallerian degeneration: gaining perspective on inflammatory events after peripheral nerve injury', Journal of Neuroinflammation, vol. 8, article 110.

Giddins, GE, Wade, PJ & Amis, AA 1989, 'Primary nerve repair: strength of repair with different gauges of nylon suture material', The Journal of Hand Surgery, vol. 14, no. 3, pp. 301-302.

Gilbert, TW, Stewart-Akers, AM, Simmons-Byrd, A & Badylak, SF 2007, 'Degradation and remodelling of small intestinal submucosa in canine Achilles tendon repair', Journal of Bone and Joint Surgery, vol. 89, no. 3, pp. 621-630.

Girdhari, RR 2017, 'The decellularized extracellular matrix in regenerative medicine', Regenerative Medicine, vol. 12, no. 5, pp. 475–477.

Griffin JW, Hogan, MV, Chhabra, AB & Deal, DN 2013 'Peripheral nerve repair and reconstruction', Journal of Bone and Joint Surgery, vol. 95, no. 23, pp. 2144-2151.

Griffin, MF, Malahias, M, Hindocha, S & Wasim, SK 2014, 'Peripheral Nerve Injury: Principles for Repair and Regeneration', Open Orthopaedics Journal, vol. 8, pp. 199–203.

Grinsell, D & Keating, CP 2014, 'Peripheral Nerve Reconstruction after Injury: A Review of Clinical and Experimental Therapies', Biomed Research International, vol. 2014.

Hargreaves, KM, Dubner, R, Brown, F, Flores, C & Joris, J 1988, 'A New and Sensitive Method for Measuring Thermal Nociception in Cutaneous Hyperalgesia', Pain, vol. 32, pp. 77-88.

Harris, ME & Tindall, SC 1991, 'Techniques of peripheral nerve repair', Neurosurgery Clinics of North America, vol. 2, no.1, pp. 93-104.

Highley, R & Sullivan, N 2013, 'Techniques in neuropathology' in Suvarna, KS, Layton, S. & Bancroft, JD (eds), *'Bancroft's Theory and Practice of Histological Techniques'*, Edinburgh, Churchill Livingstone Elsevier, pp. 358-370.

Huang, YC & Huang, YY 2006, 'Biomaterials and Strategies for Nerve Regeneration', Artificial Organs, vol. 30, no. 7, pp. 514–522.

Hulse, R, Wynick, D & Donaldson, LF 2010, 'Intact cutaneous C fibre afferent properties in mechanical and cold neuropathic allodynia', European Journal of Pain, vol. 14, no. 6, pp. 565.e1-565.e10.

Hutmacher, DW, Goh, JC & Teoh, SH 2001, 'An Introduction to Biodegradable Materials for Tissue Engineering Applications', Annals of the Academy of Medicine, vol. 30, no. 2, pp. 183-191.

Ikeda, M & Oka, Y 2012, 'The relationship between nerve conduction velocity and fiber morphology during peripheral nerve regeneration', Brain and Behavior, vol 2, no. 4, pp. 382-390.

Isaacs, J 2013, 'Major Peripheral Nerve Injuries', Hand Clinics, vol. 29, no. 3, pp. 371–382.

Jänig, W 2011, 'Mechanical allodynia generated by stimulation of unmyelinated afferent nerve fibres', Journal of Physiology, vol. 589, pp. 4407–4408.

Jankowski, MP, Lawson, JJ, Mcilwrath, SL, Rau, KK, Anderson, CE, Albers, KM, Koerber, HR 2009, 'Sensitization of cutaneous nociceptors after nerve transection and regeneration: possible role of target-derived neurotrophic factor signalling', The Journal of neuroscience, vol. 29, no. 6, pp. 1636-1647.

Jiang, X, Lim, SH, Mao, H & Chew, SY 2010, 'Current applications and future perspectives of artificial nerve conduits', Experimental Neurology, vol. 223, no. 1, pp. 86-101.

Kaemmer, D, Bozkurt, A, Otto, J, Junge, K, Klink, C, Weis, J, Sellhaus, B, O'Dey, DM, Pallua, N, Jansen, M, Schumpelick, V & Klinge, U 2010, 'Evaluation of tissue components in the

peripheral nervous system using Sirius red staining and immunohistochemistry: a comparative study (human, pig, rat)', Journal of Neuroscience Methods, vol. 190, no. 1, pp. 112-116.

Kamegaya, Y, Farinelli, WA, Vila Echague, AV, Akita, H, Gallagher, J, Flotte, TJ et al. 2005, 'Evaluation of photochemical tissue bonding for closure of skin incisions and excisions', Lasers in Surgery and Medicine, vol. 37, no. 4, pp. 264-270.

Kannan, RY, Salacinski, HJ, Butler, PE & Seifalian, AM 2005, 'Artificial nerve conduits in peripheral-nerve repair', Biotechnology and Applied Biochemistry, vol. 41, pp. 193–200.

Kaplan, HM, Mishra, P & Kohn, J 2015, 'The overwhelming use of rat models in nerve regeneration research may compromise designs of nerve guidance conduits for humans', Journal of Materials Science: Materials in Medicine, vol. 26, no. 8, p. 226.

Kiernan, JA 2007, 'Histochemistry of Staining Methods for Normal and Degenerating Myelin in the Central and Peripheral Nervous Systems', Journal of Histotechnology, vol. 30, no. 2, pp. 87-106.

Kingery, WS & Vallin, JA 1989, 'The development of chronic mechanical hyperalgesia, autotomy and collateral sprouting following sciatic nerve section in rat', Pain, vol. 38, no. 3, pp. 321-332.

Kline, DG 1982, 'Timing for exploration of nerve lesions and evaluation of the neuroma-in-continuity', Clinical Orthopaedics and Related Research, vol. 163, pp. 42-49.

Koka, R & Hadlock, TA 2001, 'Quantification of Functional Recovery Following Rat Sciatic Nerve Transection', Experimental Neurology, vol. 168, pp. 192–195.

Kokkalis, ZT, Pu, C, Small, GA, Weiser, RW, Venouziou, AI & Sotereanos, DG 2011, 'Assessment of processed porcine extracellular matrix as a protective barrier in a rabbit nerve wrap model', Journal of Reconstructive Microsurgery, vol. 27, no. 1, pp. 19-28.

Koulaxouzidis, G, Reim, G & Witzel, C 2015, 'Fibrin glue repair leads to enhanced axonal elongation during early peripheral nerve regeneration in an in vivo mouse model', Neural Regeneration Research, vol. 10, no. 7, p. 1166.

Lauto, A, Mawad, D, Barton, M, Gupta, A, Piller, SC & Hook, J 2010, 'Photochemical tissue bonding with chitosan adhesive films', BioMedical Engineering OnLine, vol. 9, p. 47.

Lauto, A, Hook, J, Doran, M, Camacho, F, Poole-Warren, LA, Avolio, A et al. 2005, 'Chitosan Adhesive for Laser Tissue Repair: In Vitro Characterization', Lasers in Surgery and Medicine, vol. 36, no. 3, pp. 193–201.

Lauto, A, Stoodley, M, Barton, M, Morley, JW, Mahns, DA, Longo, L & Mawad, D 2012, 'Fabrication and application of rose bengal-chitosan films in laser tissue repair', Journal of visualized experiments: JoVE, vol. 68.

Lee, SK & Wolfe, SW 2000, 'Peripheral nerve injury and repair', Journal of the American Academy of Orthopaedic Surgeons, vol. 8, no. 4, pp. 243–252.

Lemke, A, Penzenstadler, C, Ferguson, J, Lidinsky, D, Hopf, R, Bradl, M et al. 2017, 'A novel experimental rat model of peripheral nerve scarring that reliably mimics post-surgical complications and recurring adhesions', Disease Models & Mechanisms, vol. 10, no. 8, pp. 1015-1025.

Lun, S, Irvine, SM, Johnson, KD, Fisher, NJ, Floden, EW, Negron, L, Dempsey, SG, Mclaughlin, RJ, Vasudevamurthy, M, Ward, BR & May, BC 2010, 'A functional extracellular matrix biomaterial derived from ovine forestomach', Biomaterials, vol. 31, no. 16, pp. 4517-4529.

Lundborg, G 1987, 'Nerve regeneration and repair: A review', Acta Orthopaedica Scandinavica, vol. 58, no. 2, pp. 145-169.

Mackinnon, SE & Dellon, AL (eds) 1988, 'Surgery of the peripheral Nerve', New York, Thieme Medical Publishers.

Mackinnon, SE, Dellon, AL & O'Brien, JP 1991, 'Changes in nerve fiber numbers distal to a nerve repair in the rat sciatic nerve model', Muscle Nerve, vol. 14, no. 11, pp. 1116-1122.

Madison, RD, Archibald, SJ, Lacin, R & Krarup, C 1999, 'Factors contributing to preferential motor reinnervation in the primate peripheral nervous system', Journal of Neuroscience, vol. 19, no. 24, pp. 11007-11016.

Martins, RS, Teodoro, WR, Simplicio, H, Capellozi, VL, Siqueira, MG, Yoshinari, NH et al. 2011, 'Influence of suture on peripheral nerve regeneration and collagen production at the site of neurorrhaphy: an experimental study', Neurosurgery, vol. 68, no. 3, pp. 765-772.

Mathieu, L, Adam, C, Legagneux, J, Bruneval, P & Masmejean, E 2012, 'Reduction of neural scarring after peripheral nerve suture: An experimental study about collagen membrane and autologous vein wrapping', Chirurgie de la main, vol. 31, no. 6, pp. 311–317.

Matsuyama, T, Mackay, M & Midha, R 2000, 'Peripheral Nerve Repair and Grafting Techniques: A Review', Neurologia Medico-Chirurgica, vol. 40, no. 4, pp. 187-199.

Mavrogenis, AF, Pavlakis, K, Stamatoukou, A, Papagelopoulos, PJ, Theoharis, S, Zoubos, AB, Zhang, Z & Soucacos, PN 2008, 'Current treatment concepts for neuromas-in-continuity', Injury, vol. 39, suppl. 3, pp. 43-48.

McKerracher, L, David, S, Jackson, DL, Kottis, V, Dunn, RJ & Braun, PE 1994, 'Identification of myelin-associated glycoprotein as a major myelin-derived inhibitor of neurite growth', Neuron, vol. 13, pp. 805–811.

Menorca, RM, Fussell, TS & Elfar, JC 2013, 'Peripheral Nerve Trauma: Mechanisms of Injury and Recovery', Hand Clinics, vol. 29, no. 3, pp. 317–330.

Menovsky, T & Beek, JF 2003, 'Carbon dioxide laser-assisted nerve repair: Effect of solder and suture material on nerve regeneration in rat sciatic nerve', Microsurgery, vol. 23, no. 2, pp. 109-116.

Menovsky, T, Beek, JF 2001 ‘Laser, fibrin glue, or suture repair of peripheral nerves: A comparative functional, histological, and morphometric study in the rat sciatic nerve’, Journal of Neurosurgery, vol. 95, no. 4, pp. 694–699.

Miko, TL & Gschmeissner, SE 1994, ‘Histological Methods for Assessing Myelin Sheaths and Axons in Human Nerve Trunks’, Biotechnic & Histochemistry, vol. 69, no. 2, pp. 68-77.

Millesi, H 2006, ‘Factors affecting the outcome of peripheral nerve surgery’, Microsurgery, vol. 26, no. 4, pp. 295–302.

Montagne-clavel, J & Oliveras, JL 1996, ‘The “Plantar Test” Apparatus (Ugo Basile Biological Apparatus), a Controlled Infrared Noxious Radiant Heat Stimulus for Precise Withdrawal Latency Measurement in the Rat, as a Tool for Humans?’, Somatosensory & Motor Research, vol. 13, no. 3-04, pp. 215-223.

Mulroy, L, Kim, J, Wu, I, Scharper, P, Melki, SA, Azar, DT, Redmond, RW & Kochevar, IE 2000, ‘Photochemical keratodesmos for repair of lamellar corneal incisions’, Investigative Ophthalmology & Visual Science, vol. 41, no. 11, pp. 3335-3340.

Muratori, L, Ronchi, G, Raimondo, S, Giacobini-Robecchi, MG, Fornaro, M & Geuna, S 2012, ‘Can regenerated nerve fibers return to normal size? A long-term post-traumatic study of the rat median nerve crush injury model’, Microsurgery, vol. 32, no. 5, pp. 383-387.

Murray, JA, Willins, M & Mountain, RE 1994, ‘A comparison of absorbable and non-absorbable 10-0 sutures for the repair of a divided rat facial nerve’, Clinical Otolaryngology, vol. 19, no. 1, pp: 61-62.

Myles, LM & Glasby, MA 1991, ‘Recovery of nerve function after repair of the sciatic nerve in the rat’, Neuro-Orthopedics, vol. 12, pp. 65–84.

Navarro, X 2016, ‘Functional evaluation of peripheral nerve regeneration and target reinnervation in animal models: a critical overview’, European Journal of Neuroscience, vol. 43, no. 3, pp. 271-286.

Navarro, X & Udina, E 2009, 'Methods and protocols in peripheral nerve regeneration experimental research: Part III - Electrophysiological evaluation', International review of neurobiology, vol. 87, pp. 105-126.

Navarro, X, Vivo, M & Valero-Cabre, E 2007, 'Neural plasticity after peripheral nerve injury and regeneration', Progress in Neurobiology, vol. 82, pp. 163–201.

Ngeow, WC 2010, 'Scar less: a review of methods of scar reduction at sites of peripheral nerve repair', Oral Surgery, Oral Medicine, Oral Pathology, Oral Radiology and Endodontology, vol. 109, no. 3, pp. 357-366.

Nichols, CM, Myckatyn, TM, Rickman, SR, Fox, IK, Hadlock, T & Mackinnon, SE 2005, 'Choosing the correct functional assay: a comprehensive assessment of functional tests in the rat', Behavioural Brain Research, vol. 163, no. 2, pp. 143-158.

O'Neill, AC, Winograd, JM, Zeballos, JL, Johnson, TS, Randolph, MA, Bujold, KE 2007, 'Microvascular anastomosis using a photochemical tissue bonding technique', Lasers in Surgery and Medicine, vol. 39, no. 9, pp. 716-722.

O'Neill, AC, Randolph, MA, Bujold, KE, Kochevar, IE, Redmond, RW & Winograd, JM 2009, 'Preparation and integration of human amnion nerve conduits using a light-activated technique', Plastic and Reconstructive Surgery, vol. 124, no. 2, pp: 428-437.

Ornelas, L, Padilla, L, Di Silvio, M, Schalch, P, Esperante, S, Infante, RL, Bustamante, JC, Avalos, P, Varela, D & López, M 2006, 'Fibrin glue: an alternative technique for nerve coaptation -- Part II. Nerve regeneration and histomorphometric assessment', Journal of Reconstructive Microsurgery, vol. 22, no. 2, pp. 123-128.

Owusu, A, Mayeda, B & Isaacs, J 2014, 'Surgeon perspectives on alternative nerve repair techniques', Hand, vol. 9, no. 1, pp. 29–35.

Pabari, A, Lloyd-Hughes, H, Seifalian, A & Mosahebi, A 2014, 'Nerve conduits for peripheral nerve surgery', Plastic and Reconstructive Surgery, vol. 133, no. 6, pp. 1420–1430.

Palispis, WA & Gupta, R 2017, 'Surgical repair in humans after traumatic nerve injury provides limited functional neural regeneration in adults', Experimental Neurology, vol. 290, pp. 106-114.

Palmgren, A 1960, 'Specific Silver Staining of Nerve Fibres', Acta Zoologica, vol. 41, no. 3, pp. 239–265.

Panagopoulos, GN, Megaloikonomos, PD & Mavrogenis, AF 2017, 'The Present and Future for Peripheral Nerve Regeneration', Orthopedics, vol. 40, no. 1, pp. 141-156.

Parmaksiz, M, Dogan, A, Odabas, S, Elçin, AE & Elçin, YM 2016, 'Clinical applications of decellularized extracellular matrices for tissue engineering and regenerative medicine', Biomedical Materials, vol. 11, no. 2.

Pilling, D, Fan, T, Huang, D, Kaul, B & Gomer, RH 2009, 'Identification of Markers that Distinguish Monocyte-Derived Fibrocytes from Monocytes, Macrophages, and Fibroblasts', PLos One, vol.4, no. 10, pp. e7475.

Pinho, AC, Fonseca, AC, Serra, AC, Santos, JD & Coelho, JF 2016, 'Peripheral Nerve Regeneration: Current Status and New Strategies Using Polymeric Materials', Advanced Healthcare Materials, vol. 5, no. 21, pp. 2732-2744.

Rijal, G 2017, 'The decellularized extracellular matrix in regenerative medicine', Regenerative Medicine, vol. 12, no. 5, pp. 475-477.

Robinson, LR 2000, 'Traumatic injury to peripheral nerves', Muscle & Nerve, vol 23, no. 6, pp. 863–873.

Rodríguez-Vázquez, M, Vega-Ruiz, B, Ramos-Zúñiga, R, Saldaña-Koppel, DA & Quiñones-Olvera, LF 2015, 'Chitosan and Its Potential Use as a Scaffold for Tissue Engineering in Regenerative Medicine', BioMed Research International, vol. 2015.

Rotshenker, S 2011, 'Wallerian degeneration: the innate-immune response to traumatic nerve injury', Journal of Neuroinflammation, vol. 8, article 109.

Rupp, A, Dornseifer, U, Fischer, A, Schmahl, W, Rodenacker, K, Jütting, U, Gais, P, Biemer, E, Papadopulos, N & Matiasek, K 2007, 'Electrophysiologic assessment of sciatic nerve regeneration in the rat: Surrounding limb muscles feature strongly in recordings from the gastrocnemius muscle', Journal of Neuroscience Methods, vol. 166, no. 2, pp. 266-277.

Sameem, M, Wood, TJ & Bain, JR 2011, 'A Systematic Review on the Use of Fibrin Glue for Peripheral Nerve Repair', Plastic and Reconstructive Surgery, vol. 127, pp. 2381-2389.

Saied, A, Shekaari, MA, Sadeghifar, A & Karbalaeikhani, A 2015, 'Introduction of a New Suture Method in Repair of Peripheral Nerves Injured with a Sharp Mechanism', The Archives of Bone and Joint Surgery, vol. 3, no. 4, pp. 254-259.

Schmalbruch, H 1986, 'Fiber composition of the rat sciatic nerve', The Anatomical Record, vol. 215, pp. 71-81.

Schmalbruch, H, Al-Amood, WS & Lewis, DM 1991, 'Morphology of long-term denervated rat soleus muscle and the effect of chronic electrical stimulation', Journal of Physiology, vol. 441, pp. 233–241.

Schmidhammer, R, Zandieh, S, Hopf, R, Mizner, I, Pelinka, LE, Kroepfl, A & Redl, H 2004, 'Alleviated tension at the repair site enhances functional regeneration: the effect of full range of motion mobilization on the regeneration of peripheral nerves--histologic, electrophysiologic, and functional results in a rat model', The Journal of Trauma, vol. 56, no. 3, pp. 571-84.

Schwab, ME 1996, 'Molecules inhibiting neurite growth: a minireview', Neurochemical Research, vol. 21, pp. 755-761.

Seddon, HJ 1975, Surgical disorders of the peripheral nerves, New York, Churchill Livingstone, pp. 21–23.

Shaikh, S, Shortland, P, Lauto, A, Barton, M, Morley, JW & Mahns, DA 2016, 'Sensory perturbations using suture and sutureless repair of transected median nerve in rats', Somatosensory & Motor Research, vol. 33, no. 1, pp. 20-28.

Shen, YI, Redmond, SL, Papadimitriou, JM, The, BM, Yan, S, Wang, Y 2014, 'The biocompatibility of silk fibroin and acellular collagen scaffolds for tissue engineering in the ear', Biomedical Materials, vol. 9, no. 1.

Siemionow, M. & Brzezicki, G 2009, 'Current techniques and concepts in peripheral nerve repair', International Review of Neurobiology, vol. 87, pp. 141-172.

Sunderland, S 1951, 'A classification of peripheral nerve injuries producing loss of function', Brain, vol 74, pp. 491-516.

Suri, A, Mehta, VS & Sarkar, C 2002, 'Microneural anastomosis with fibrin glue: an experimental study', Neurology India, vol. 50, no. 1, pp. 23-26.

Temple, CL, Ross, DC, Dunning, CE, Johnson, JA 2004, 'Resistance to disruption and gapping of peripheral nerve repairs: An in vitro biomechanical assessment of techniques', Journal of Reconstructive Microsurgery, vol. 20, no. 8, pp. 645–650.

Terzis, J, Faibisoff, B & Williams, B 1975, 'The nerve gap: suture under tension vs. graft', Plastic and reconstructive surgery, vol. 56, no. 2, pp. 166-170

Thalhammer, JG, Vladimirova, M, Bershad-Sky, B & Strichartz, GR 1995, 'Neurologic evaluation of the rat during sciatic nerve block with lidocaine', Anaesthesiology, vol. 82, pp. 1013-1025.

Tos, P, Crosio, A, Pugliese, P & Adani, R, Toia, F & Artiaco, S 2015, 'Painful scar neuropathy: principles of diagnosis and treatment', Plastic and Aesthetic Research, vol. 2, no. 4, pp. 158-164.

Valero-Cabré, A, Tsironis, K, Skouras, E, Navarro, X & Neiss, W 2004, 'Peripheral and Spinal Motor Reorganization after Nerve Injury and Repair', Journal of Neurotrauma, vol. 21, no. 1, pp. 95-108.

Vogelaar, CF, Vrinten, DH, Hoekman, MF, Brakkee, JH, Burbach, JP & Hamers, FP 2004, 'Sciatic nerve regeneration in mice and rats: recovery of sensory innervation is followed by a slowly retreating neuropathic pain-like syndrome', Brain Research, vol. 1027, pp. 67–72.

Wang, YM, Sunitha, MP & Chung, KC 2013, 'How to Measure Outcomes of Peripheral Nerve Surgery', Hand Clinics, vol. 29, no. 3, pp. 349–361.

Webster, A, Britton, D, Apap-Bologna, A & Kemp, G 1989, 'A dye-photosensitized reaction that generates stable protein–protein crosslinks', Analytical Biochemistry, vol. 179, no. 1, pp. 154-157.

Whitlock, EL, Kasukurthi, R, Yan, Y, Tung, TH, Hunter, DA & Mackinnon, SE 2010, 'Fibrin glue mitigates the learning curve of microneurosurgical repair', Microsurgery, vol. 30, no. 3, pp. 218-222.

Wood, MD, Kemp, SW, Weber, C, Borschel, GH & Gordon, T 2011, 'Outcome measures of peripheral nerve regeneration', Annals of Anatomy, vol. 193, no. 4, pp. 321–333.

Wu, P, Chawla, A, Spinner, RJ, Yu, C, Yaszemski, MJ, Windebank, AJ & Wang, H 2014, 'Key changes in denervated muscles and their impact on regeneration and reinnervation', Neural Regeneration Research, vol. 15, no. 20, pp. 1796-1809.

Xu, N, Yao, M, Farinelli, W, Hajjarian, Z, Wang, Y, Redmond, RW & Kochevar, IE 2015, 'Light-activated sealing of skin wounds', Lasers in Surgery and Medicine, vol. 47, pp. 17–29.

Yang, P, Yao, M, Demartelaere, SL, Redmond, RW & Kochevar, IE 2012, 'Light-activated sutureless closure of wounds in thin skin', Lasers in Surgery and Medicine, vol. 44, no. 2, pp. 163-167.

Yao, M, Yaroslavsky, A, Henry, FP, Redmond, RW & Kochevar, IE 2010, 'Phototoxicity is not associated with photochemical tissue bonding of skin', Lasers in Surgery and Medicine, vol. 42, no. 2, pp. 123-131.

Yeomans, DC & Proudfit, HK 1994, 'Characterization of the Foot Withdrawal Response to Noxious Radiant Heat in the Rat', Pain, vol. 59, pp. 85-97.

Yi, C & Dahlin, LB 2010, 'Impaired nerve regeneration and Schwann cell activation after repair with tension', Neuroreport, vol. 21, no. 14, pp. 958–962.

Zigmond, RE & Echevarria, FD 2019, 'Macrophage biology in the peripheral nervous system after injury', Progress in Neurobiology, vol. 173, pp. 102-121.